Recent Progress in Micro-LED-Based Display Technologies

Abdur Rehman Anwar,* Muhammad T. Sajjad,* Muhammad Ali Johar,*
Carlos A. Hernández-Gutiérrez, Muhammad Usman, and S. P. Łepkowski

The demand for high-performance displays is continuously increasing because of their wide range of applications in smart devices (smartphones/watches), augmented reality, virtual reality, and naked eye 3D projection. High-resolution, transparent, and flexible displays are the main types of display to be used in future. In the above scenario, the micro-LEDs (light-emitting diodes) display which has outstanding features, such as low power consumption, wider color gamut, longer lifetime, and short response-time, can replace traditional liquid crystal displays and organic LEDs-based display technologies. However, to attain a remarkable position in future display technology, the micro-LEDs need to overcome problems associated with mass transfer and its high cost of manufacturing. Besides micro-LEDs, the other option for future displays includes the usage of color conversion medium (phosphor/ quantum dots) to convert some of the blue light into other colors. In this review, the various mass transfer display technologies and color conversion strategies which are being used for the realization of a full-color display are discussed.

A. R. Anwar, S. P. Łepkowski
Institute of High-Pressure Physics - Unipress
Polish Academy of Sciences
ul. Sokołowska 29/37, Warszawa 01-142, Poland
E-mail: aranwar@unipress.waw.pl

M. T. Sajjad
London Centre for Energy Engineering (LCEE), School of Engineering
London South Bank University
103 Borough Road, London SE1 0AA, UK
E-mail: sajjadt@lsbu.ac.uk

M. A. Johar
Holonyak Micro and Nanotechnology Laboratory
University of Illinois at Urbana-Champaign
Champaign, IL 61801, USA
E-mail: johar@illinois.edu

C. A. Hernández-Gutiérrez
Tecnológico Nacional de México/Instituto Tecnológico de Tuxtla Gutiérrez
Grupo de Optomecatrónica
Carretera Panamericana km 1080, Tuxtla Gutiérrez C.P. 29050, México
E-mail: carlos.hg@tuxtla.tecnm.mx

M. Usman
Faculty of Engineering Sciences
Ghulam Ishaq Khan Institute of Engineering Sciences and Technology
Topi, Khyber Pakhtunkhwa 23460, Pakistan

1. Introduction

With the advancement in technology, the use of "display technology" in our daily life is increasing abruptly because of its broad range of applications such as televisions, desktop monitors, smartphones health care devices, and data projectors.[1–4] In display technology, the very first cathode ray tube (CRT)-based color television was introduced in 1940s, leading to the first color broadcast in 1954. The design of CRT is comprised of the vacuum tube having an electron gun which generates the beam of guided electrons which is then directed toward the specially designed screen to emit primary colors, i.e., red, green, and blue (RGB).[5] Because of their prominent features such as good response rate and best visual depth, CRT-based televisions have gained splendid popularity in the display industry for nearly four decades, from 1950s to 1990s. In 2000s, the liquid crystal display (LCD) was successfully introduced as an alternative to CRT technology.[6]

LCD is a nonemissive technology where a unit of backlight source is used to create light propagation through a liquid crystal panel (the polarizer absorbs ≈50% of the incident light) and then color filters are used to convert this mixture of white light into perfect red, green, and blue color.[7] The LCD technology gained significant attention because of its high-power efficiency and portability. In CRT technology, portability is one of the major drawbacks. Albeit LCD technology faced serious issues in the perspective of color saturation, response time, and conversion efficiency.[8] To improve their performance, materials with high color saturation and better response time and upgraded backlight unit with better conversion efficiency were used.[9,10] These modifications improved optical efficiency and color gamut of LCD, however, two-thirds of light generated is still being wasted. In 1990s, organic light-emitting diodes (OLEDs) were introduced to display technology.[11] The OLEDs are efficient power-saving devices, have a high response rate and broad viewing angle, and do not need an extra backlight unit in them.[12,13] They have been widely used in smart electronic products such as foldable and curved displays because of their prominent features of transparency and perfect flexibility.[14] However, the OLEDs faced cumbersome issues of their shorter device lifetime and inefficient color purity which is limiting its application in displays.[15] In short, both technologies (LCDs and OLEDs) have some critical issues which need to be addressed for their

**ADVANCED
SCIENCE NEWS**

www.advancedsciencenews.com

LASER
& PHOTONICS
REVIEWS

www.lpr-journal.org

successful utilization in future smart displays.[16,17] Recently, the inorganic material-based light-emitting diodes (LEDs) with the lateral dimension down to less than 100 μm × 100 μm (which is also called micro-LEDs) have attained much more attention for a display technology[18–20] due to their distinguished features such as lower power consumption (30–40% of LCD), longer life span, the quick response time (nanosecond level), and wide RGB color gamut.[21,22] In comparison to the already existing LCD, the micro-LED display has a ten times faster response rate, 1.4 times broader color gamut, and 3.5 times higher contrast ratio.[23] Further improvements in luminescence efficiency of these micro-LEDs were achieved by enhancing light extraction efficiency, e.g., Choi et al. have introduced the concept of micropillar geometry by patterning the micropillars on LED mesa with diameters ranging from 4 to 20 μm. The device with a pillar diameter of 4 μm showed better performance compared to larger diameters. This performance improvement was attributed to strain relaxation (reduction of piezoelectric field), minimum self-heating (which degrade their performance), and also to proper current spreading across the device.[24,25] Recently, Bower et al. have demonstrated a variety of prototype passive-matrix and micro-IC-driven active-matrix displays utilizing both lateral and flip-chip micro-LEDs.[26]

The micro-LEDs-based display technology has also attracted significant attention from investors and companies.[27] In 2012, Sony introduced its first micro-LED-based television panel (55 in.) which has six million micro-LEDs.[23] After that, in 2018, LG successfully presented micro-LEDs-based large (175 in.) display. Samsung, also in 2018, launched 146 in. micro-LEDs-based television. In the same year, PlayNitride stepped in toward micro-LED-based display technology by introducing 0.89 in. 64 × 64 panels (105 pixels per inch) and another 3.12 in. 256 × 256 panels (116 pixels per inch) full-color display. Another company, X-Celeprint has also introduced 5.1 in. micro-LED-based display which was comprised of 8 × 15 μm RGB LEDs having 70 pixels per inch. In 2020, numerous companies including Lumiode, Jade Bird Display, and Plessey have announced the launching of their product soon.[21]

Mostly, phosphors have been used as color converters to achieve full color micro-LEDs. However, recently, the color conversion of the micro-LEDs has also been improved using quantum dots (QDs) and nanoparticles.[28,29] Apart from displays, micro-LEDs have been employed to achieve high-speed as well as long-distance visible light communication.[30,31]

A sudden efficiency degradation is normally seen by decreasing the dimension of devices from LEDs to micro-LEDs. In this review, we discussed the problems associated with the epitaxial growth of micro-LEDs which lead to these efficiency degradations and compared the various technologies for the mass production of micro-LEDs. We also discussed the phosphor and QD-based color conversion technologies with their positive and negative aspects for full color display. Finally, we listed some prominent strategies which could be useful to overcome the problems associated with color conversion technology.

2. Epitaxial Growth and Chip Processing of LEDs

The III-V-based LEDs is widely being used in a variety of applications. To meet the demand of the market and decrease the manufacturing cost, the industry is moving from 2 in. to 4 and 6 in. wafer sizes.[32,33] Although, sapphire remains the dominant substrate material for the epitaxy of nitrides LEDs, because it allows lower dislocations densities and the best crystalline quality.[34] But the use of large Si substrates also attracts great interest due to its availability in the market at a lower cost. Further, the growth over Si could be useful to integrate nitrides with silicon standard electronics.[35,36] However, Si is known to have high chemical reactivity toward other elements, e.g., gallium is reported to form an alloy with Si which further makes GaN-on-Si challenging. Si has also been known to diffuse into GaN causing n-type conductivity.[37] An additional layer such as Al, GaAs, etc., thus, has been traditionally used between GaN and Si.[38,39] Another challenge is that opaque silicon leads to around 80% unwanted light absorption.[40] Further, it is also challenging to achieve crack-free GaN-on-Si for efficient micro-LEDs.[41]

Normally, the metal-organic chemical vapor deposition technique is utilized for the fabrication of InGaN/GaN-based LEDs. The layers are grown along the c-plane [0001] on the sapphire (Al_2O_3) or silicon (Si [111]) substrate.[42–44] Then, the p-contact layer is grown over the active region (InGaN/GaN) which is usually indium tin oxide for better current spreading and also to achieve an ohmic contact.[45,46] By the etching process, the LED mesa is defined, and is etched down to the n-doped GaN layer. Finally, n and p electrodes are deposited by utilizing the beam evaporation technique.[47,48] The chip size of conventional LEDs (for traditional solid-state lighting) is of the order of hundred microns to a few millimeters. The fabrication processes of micro-LEDs are the same as mentioned above for conventional LEDs, except for the smaller size of an LED mesa. As the size of the LED mesa is reduced to tens of microns, it poses a serious challenge to the LED epitaxy (and leads to more defects). Therefore, the performance of micro-LEDs is more degraded in comparison to conventional LEDs. These defects provide paths for reverse current leakage (surface leakage current) in the device.[49] In conventional LEDs, the external quantum efficiency (EQE) is not affected by these factors because the density of dislocation defects are low (≈10^8 cm^{-2}) compared to micro-LED.[50] For successful epitaxial growth of gallium nitride (GaN)-based micro-LEDs, low defect density, single-wavelength light emission, and uniform spreading of driving current are required.[51] To meet the requirement of large-scale micro-LEDs, a sapphire substrate with a large dimension is also required. Larger substrate dimension leads to higher thermal and lattice mismatch with the epitaxial LED layer.[52,53] The thermal mismatch at a surface can lead to the nonuniform distribution of indium content in the InGaN/GaN multi-quantum wells (MQWs) wafer. Basically, the difference in temperature of 1 °C at a surface could induce a shift in emission wavelength of ≈1.8 nm in the case of blue LEDs and 2.5 nm in the case of green LEDs.[54,55] To address these problems, a number of solutions have been proposed, e.g., Lu et al. reported the uniform emission with ≈2 nm deviation by implementing the proper pocket design for 2, 4, and 6 in. wafer.[53] Aida et al. have reported GaN on the sapphire substrate with reduced bowing in the wafer by utilizing laser processing for stress implantation.[56]

With the decrease in size from LED to micro-LED, both chip fabrication and their performance are greatly affected. This is due to the enhanced density of surface defects because of the sidewall effect. Normally defects cause the nonradiative recombination (Shockley–Read–Hall (SRH) recombination) to occur.[57]
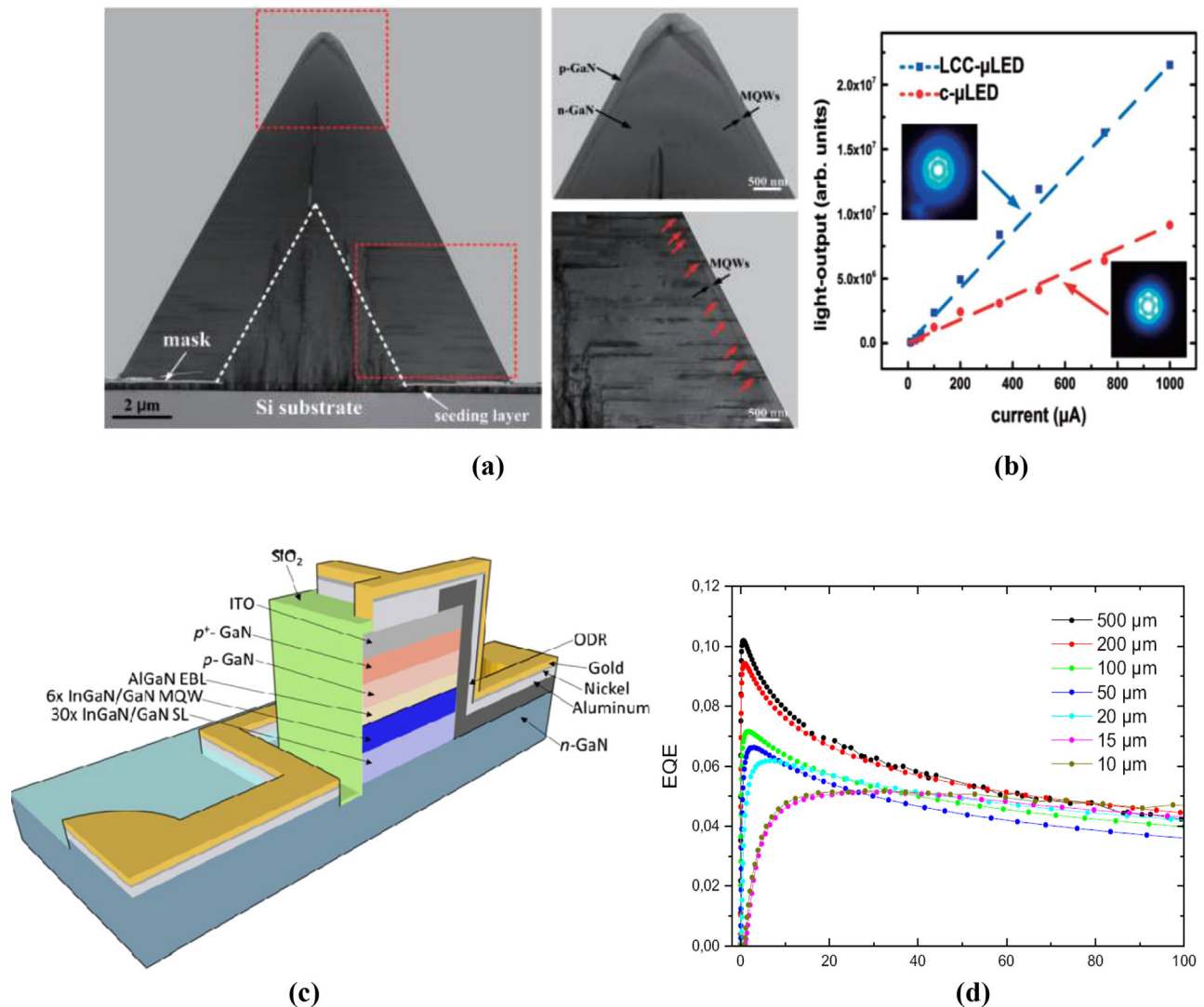
**ADVANCED
SCIENCE NEWS**

www.advancedsciencenews.com

LASER
& PHOTONICS
REVIEWS

www.lpr-journal.org

Figure 1. a) Cross-sectional and magnified TEM image of a pyramidal μ-LED structure, the detail of the structure, i.e., n-GaN, MQWs, and p-GaN is shown in magnified image with black arrow. b) Comparison of light output power as a function of injection current (inset showing light-emitting images collected at an injection current of 15 μA). Reproduced with permission.[65] Copyright 2015, The Japan Society of Applied Physics. c) Schematic diagram of μ-LED with sidewall passivation layer by using ALD. Reproduced with permission.[66] Copyright 2018, Optical Society of America, and d) effect of chip size on EQE as a function of current density (A/cm^2). Reproduced with permission.[49] Copyright 2016, Elsevier publishing.

Due to these SRH recombination centers, the internal quantum efficiency of the device is reported to decrease at low current density whereas, for high current density, the effect of current crowding dominates in the device. Such defects can be reduced via thermal annealing.

Generally, the InGaN alloys have a lower surface recombination rate (102–104 cm s^{-1}) in comparison to AlGaInP, therefore InGaN LEDs have comparatively higher EQE.[58] The sidewall recombination which is also called SRH nonradiative recombination caused by plasma dry etching originates from the higher surface to volume ratio. The primary channels of carrier losses are surface recombination velocity and carrier diffusion length. Bulashevich and Karpov found that narrow bandgap and zinc blende crystal structures have relatively higher values than those of wurtzite crystal structures such as GaN and InGaN.[59] Hence,

as the chip size is reduced, the nonradiative recombination at the sidewalls of the active region in the case of AlGaInP-based μ-LEDs is enhanced which then has a detrimental influence on their efficiencies. On the other hand, Li et al. reported nearly size-independent EQE in the case of InGaN-based μ-LEDs due to very low surface recombination.[60]

A comparison between the chip size and EQE is given in **Figure 1**d which shows that the decrease in chip size from 500 μm × 500 μm to 10 μm × 10 μm led to a reduction in the EQE from ≈10% to 5%.[49,61,62] To solve this problem, numerous strategies are reported.[63,64] We have included a few of them here, e.g., Chen et al. have reported pyramidal micro-LED, in which reverse current leakage was minimized by a factor of two by employing SiO₂ current confinement layer as shown in Figure 1a.[65] Consequently, the light output power was enhanced approximately

**ADVANCED
SCIENCE NEWS**

www.advancedsciencenews.com

LASER
& PHOTONICS
REVIEWS

www.lpr-journal.org

Table 1. Comparison of various mass transfer technologies. The detail about performance (transfer rate) for each mass transfer technology is given in refs. [27,86] and chip size in ref. [63].

Transfer method	Performance	Advantages	Disadvantages	Chip size	Used by companies
Laser-based	Transfer yield 99.99%. The transfer rate is ≈100 million per hour.	No impurities transfer on substrate surface.	Laser source can damage their transfer stability.	>1 μm	Optovate/Uniqarta[78]
Electrostatic	The transfer rate is ≈1 million per hour.	Flexible to use and have perfect repeatability.	Due to electrostatic, the charges are induced which can degrade device performance	1–100 μm	Apple/Luxvue[84]
Fluidic-based assembly	Transfer yield ≈65%. The transfer rate is ≈50 million per hour.	Economical, easy to operate and minimum parasitic effect.[21]	Inefficient, the probability of pixel damages during transfer is high.	>20 μm	Foxconn/eLux[87]
Elastomer stamp (van der Waals)	Transfer yield 99.99%. The transfer rate is ≈1 million per hour.	It can be transferred by efficient and economical way because of its stickiness (elastomer stamp) nature.	It has poor repeatability because the stamp adhesion force is controlled by peeling speed. It is optimized by a magnetorheological stamp.[88]	>10 μm	X-Celeprint[89]
Roll-to-Roll/R2R	Transfer yield 99.99%. The transfer rate is ≈10 000 per second.	Economical, high efficiency and high throughput	Probability of device damages is high.	≈less than 100 μm[27]	Korean institute of machinery and materials[90,91]

more than twice (Figure 1b). Wong et al. have introduced the SiO$_2$ layer for sidewall passivation (Figure 1c)[66] which led to 37.5% enhancement in the EQE of micro-LED (with a dimension of 20 μm × 20 μm).

3. Assembling Technologies for Mass Production of Micro-LEDs Display

Despite their tremendous performance, this technology has faced a lot of problems in their high commercial production. The problems such as monolithic fabrication, mass transfer of micro-LEDs chips, and full-color realization have limited their successful mass production.[67–69] Normally, in inorganic LEDs, the dimension of developed wafers is usually 4, 6, and 8 in.[70] Because of this, it is compulsory to utilize mass transfer technology for large area micro-LED displays by shifting the LED array to a receiver substrate. In parallel to mass transfer technology, pick and place, selective release and transfer, and self-assembly have also been utilized for shifting the LED array on a substrate.[21,71,72] Each technology has its own advantages and disadvantages and can impact the performance of the display. For example, in order to realize a 3840 × 2160 × 3 micro-LED full-color display consisting of 4 K pixels per inch, nearly 2488 pixels must be destroyed after transmission for 99.99% reliable transmission technology.[63,73] The manufacturing companies have introduced some approaches such as electrostatic,[74,75] laser-based,[76–78] van der Waals,[3,79,80] and fluidic-based assembly[81–83] for efficient transfer. **Table 1** shows the comparison of different mass transfer technologies in the aspect of their advantages/disadvantages, transfer yield, and transfer rate.

The electrostatic-based mass transfer technology was introduced by the Apple Co.-owned company "LuxVue" in 2012. They successfully realized a micro device array by utilizing this technology.[84] The transfer of an LED chip from a host substrate to a receiving substrate is done using an electrostatically charged transfer stamp/target substrate. By applying a voltage, the elec-

trostatic transfer head array picks up micro device array from the host substrate via charge adsorption force. Then, the receiving substrate is brought into contact with a micro device array. Meanwhile, the applied voltage on the electrostatic transfer head is removed. The transfer is flexible because it can selectively transfer each component, i.e., the pitch of electrostatic head array and pitch of the micro-LED on the receiving substrate. But the applied voltage to the head during the electrostatic induction can produce a charging phenomenon that can damage the micro devices (e.g., micro-LEDs).[21] Therefore, careful control of the voltage is very important during the transfer.

Laser-based transfer technique (laser-induced forward transfer) utilizes laser beams to detach the micro-LEDs from the carrier substrate and then shifts them toward the receiver substrate.[85] Like the laser-lift-off technique, laser beam irradiation causes ablation at the interface of substrate/LED to detach the chip from the carrier substrate and, in the meantime generates a force to push the chip toward the receiver substrate. In 2013, Uniqarta introduced massively parallel laser-enabled technology (MPLET) for large-scale transfer of micro-LEDs.[78] The micro-LEDs were deposited on the substrate (glass) plated with a dynamic release layer (DRL). When a UV beam irradiates the targeted area of a substrate, bubbles was generated between the substrate and DRL. Under the action of bubbles expansion and gravity, the micro-LEDs were shifted toward the receiver substrate with a pitch of 10–300 μm. MPLET technology utilizes a diffractive optical element to diffract a single beam into the multiple sub-beams. Each sub-beam corresponds to the transfer of a micro-LED. By utilizing MPLET, Marinov successfully shifted micro-LEDs with an average placement error of 1.8 μm at a high transfer speed of more than 100 M units h^{-1}.[78]

Rogers group used the elastomer stamp to initially develop micro-transfer printing technology (μTP).[79,92] In μTP, the transfer of the micro-LEDs from one substrate to another was performed using the difference in adhesion between the stamp and the substrate. For picking (donor substrate) and placing (recep-

**ADVANCED
SCIENCE NEWS**

www.advancedsciencenews.com

LASER
& PHOTONICS
REVIEWS

www.lpr-journal.org

tor substrate) of the stamp, the peeling speed is very important. The peeling speed of ≈ 10 cm s^{-1} is generally used for pulling the stamp away from the donor substrate which can generate effective adhesive force between the stamp and micro-LEDs. Whereas, the peeling speed of ≈ 1 mm s^{-1} is usually used for placing the micro-LEDs on a receptor substrate (i.e., by decreasing the peeling speed, the adhesive force is also reduced).[86] The stamp, used to pick and transfer the micro-LEDs, is made up of soft and elastic materials normally the major portion is made up of polydimethylsiloxane and shape memory polymers.[93] Because of its excellent nature of stickiness and flexibility, it is suitable to transfer technology for curved screens and wearable applications. In 2017, Radauscher et al. used this technology to develop active and passive color micro-LED arrays and showed a high transfer yield of $\approx 99.99\%$.[94] There are also reports where poor repeatability of this method is reported due to the dependence of adhesion force on the peeling speed.[88] To address this problem, Kim et al. in 2019 used magnetorheological stamps and controlled the adhesion force by the varying magnetic field during the pick and place.[88] In 2020, Lu et al. optimized the stamp transfer technology by utilizing the support vector model.[95] The placement rate of ≈ 1 M units h^{-1} was achieved using a stamp size of 150 mm. This is suitable for a small area or finer micro-LEDs display applications but not enough for large area displays.[86]

The fluidic-based assembly is cost-effective technology and can be used to transfer the large-spacing micro-LEDs. This technology can easily manage microstructures (e.g., micro-LEDs) on a large area substrate with high throughput. Moreover, the interconnection parasitic effect is low in comparison to other available transfer methods.[21,96] In this technology, the target substrate, micro-LEDs, and transfer components are immersed in liquid (e.g., isopropanol, acetone, or distilled water). This liquid is then utilized as a medium to connect the chip and target substrate electrically and mechanically. The fluidic assembly uses gravity and surface tension as a driving force to drive and capture the micro-LEDs on a target substrate. After being positioned on the substrate, the anode and cathodes electrodes are bonded with the driver ICs for electrical connections.[27,87] In 1994, Yeh and Smith performed the transfer of trapezoidal-shaped GaAs LED devices from a growth wafer to a Si substrate via this technology.[82] Later in 2007, Saeedi et al. utilized this technology to transfer the micro-LEDs grown on AlGaAs to a flexible substrate with a yield of $\approx 65\%$.[97] In 2017, Sasaki et al. reported fluidic assembly technology for the massive parallel assembly of micro-LEDs.[81] In 2019, Cho et al. demonstrated high yield fluidic assembly technology for GaN microchips for display applications, where, they precisely assembled more than 19 000 blue GaN-microchips with 45 µm in diameter at 99.90% yield within 1 min.[98] Despite these successes, this technology is not mature yet and still needs to be flourished (in the perspective of low melting temperature alloys which damage the chip performance) further for commercial usage.

Another transfer approach "roll-to-roll (roll-to-plate)" was developed by the Korean Institute of Machinery and Materials (KIMM).[90,91] This can be used to shift micro-LEDs with a chip size and thickness below 100 µm and 10 µm, respectively. This technique can provide a high transfer rate of $\approx 10\,000$ devices per second for lightweight, flexible, and stretchable displays. For this, the chips need to be transferred to the roller, and then the rotation

between the rollers is used to imprint the chip onto a target substrate. The advantage of this approach is that the same method is used to pick up the thin-film transistor (electronic components) and LED components and place them on the desired substrate. Therefore, this process increases the production speed.[99] However, it cannot selectively transfer micro-LEDs. Further, precision and reliability are also difficult to guarantee.

Among the above-mentioned mass transfer technologies (in Table 1), the elastomer stamp (van der Waals interaction) is most frequently used[68,89,101] because of its unique feature (e.g., stickiness) which can be easily transferred to the receiver substrate with 99.99% transfer yield.[102] Comparatively, laser-based and electrostatic technologies have good repeatability which greatly reduces their mass transfer cost, whereas the poor repeatability was the negative point of elastomer technology which can be improved by introducing a magnetorheological stamp (electromagnetic in the nutshell, the elastomer stamp (van der Waals interaction) is the promising technology for the small devices).[99] Moreover, the replacement of the stamp head with an electromagnetic-based head is considered a prominent solution for the enhancement of cost effectiveness and reliability of transfer. However, for the realization of a large-size display of micro-LED, the roll-to-roll technology has advantage because of its high throughput. The schematic working diagram of the mass transfer technologies is shown in **Figure 2**a–d.

4. Color Conversion Technology for RGB Display

In full color micro-LED display, each pixel contains three primary colors (red, green, and blue) that can be combined to produce the required color. To achieve the different combinations of RGB colors, the different biases (current) are applied to control each (red/green/blue) LED. However, in LCD technology, each pixel contains color filters and liquid crystals (light switches). The required color is generated by passing the light from the backlight unit through each pixel. Normally, the III–V group materials (In-GaN/GaN) are used to produce a single wavelength (monochromatic) emission source.[103–105] However, there is a critical challenge for the researchers to develop an approach to achieve full-color micro-LED-based display from single color LED.[106,107]

The emission wavelength of InGaN/GaN MQW LEDs can be changed from blue to red through the variations of indium content.[108] Comparative to blue GaN-based LEDs, the luminescence efficiency of green and red LEDs is not only very low[105,109] but also decreases abruptly with the increase in operating current density.[110] This is mainly due to the lattice mismatch between InGaN and GaN layers which leads to misfit strain. The large lattice mismatch between InN and GaN(reaching $\approx 11\%$) is the main factor limiting the growth of high-quality indium-rich InGaN/GaN QWs.[111–113] The biaxial compressive strain hinders the incorporation of In atoms in the InGaN lattice, thus causing the so-called compositional pulling effect.[111,112] An accumulation of large strain in InGaN/GaN QWs can also lead to the generation of defects, which act as nonradiative recombination centers and can reduce the EQE.[113,114] In order to achieve the emission in green and red spectral regions, one can try to exploit the quantum-confined Stark effect (QCSE) which occurs in the c-plane of InGaN/GaN QWs.[115] Due to the presence of the built-in electric field in these structures,
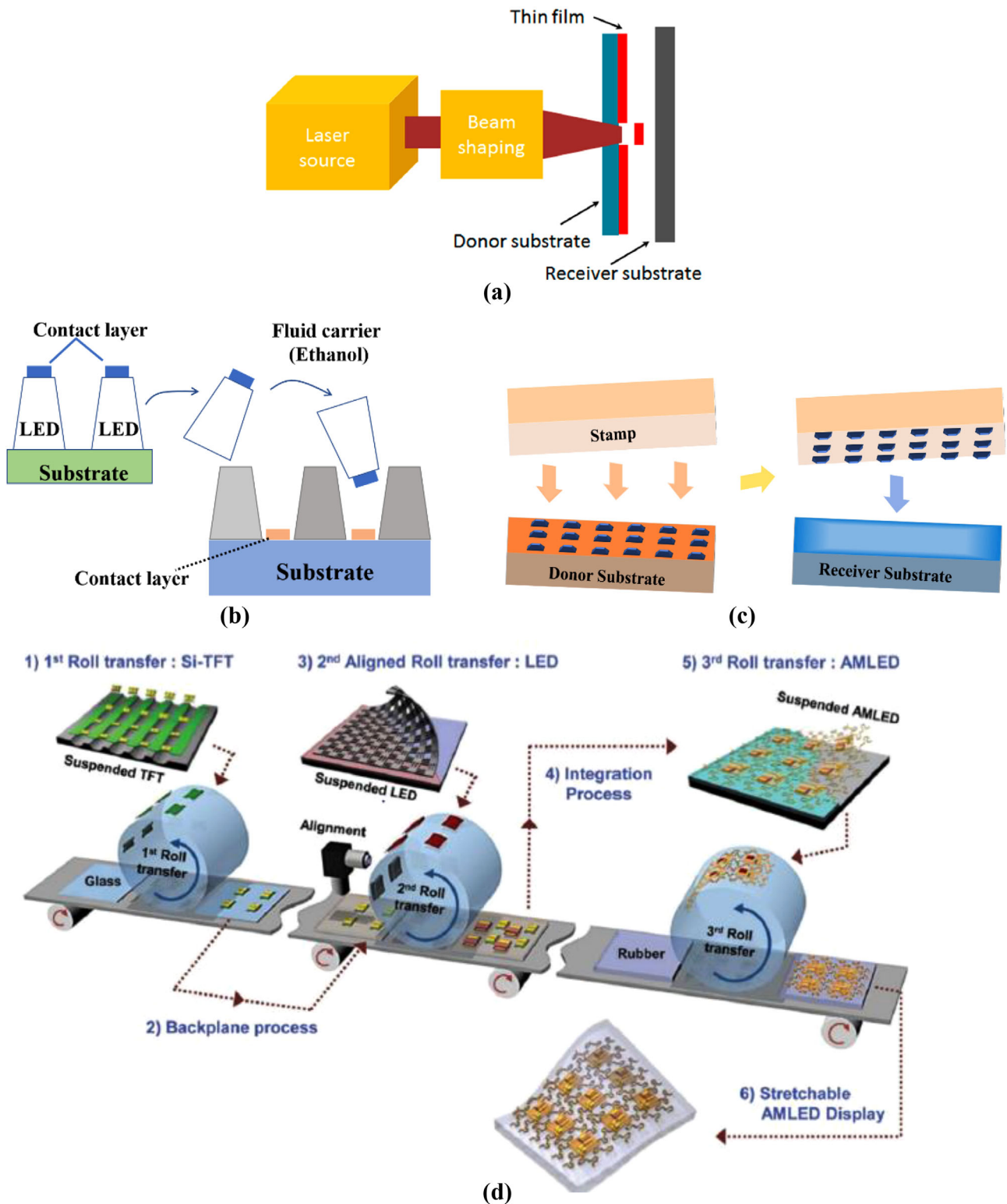
ADVANCED
SCIENCE NEWS

www.advancedsciencenews.com

LASER
& PHOTONICS
REVIEWS

www.lpr-journal.org

Figure 2. Schematic diagram of a) laser-induced forward transfer process. Reproduced with permission.[85] Copyright 2015, Elsevier publishing. b) Fluidic-based assembly, c) elastomer stamp, d) roll-to-roll/R2R assembly. Reproduced with permission.[100] Copyright 2017, John Wiley and Sons.
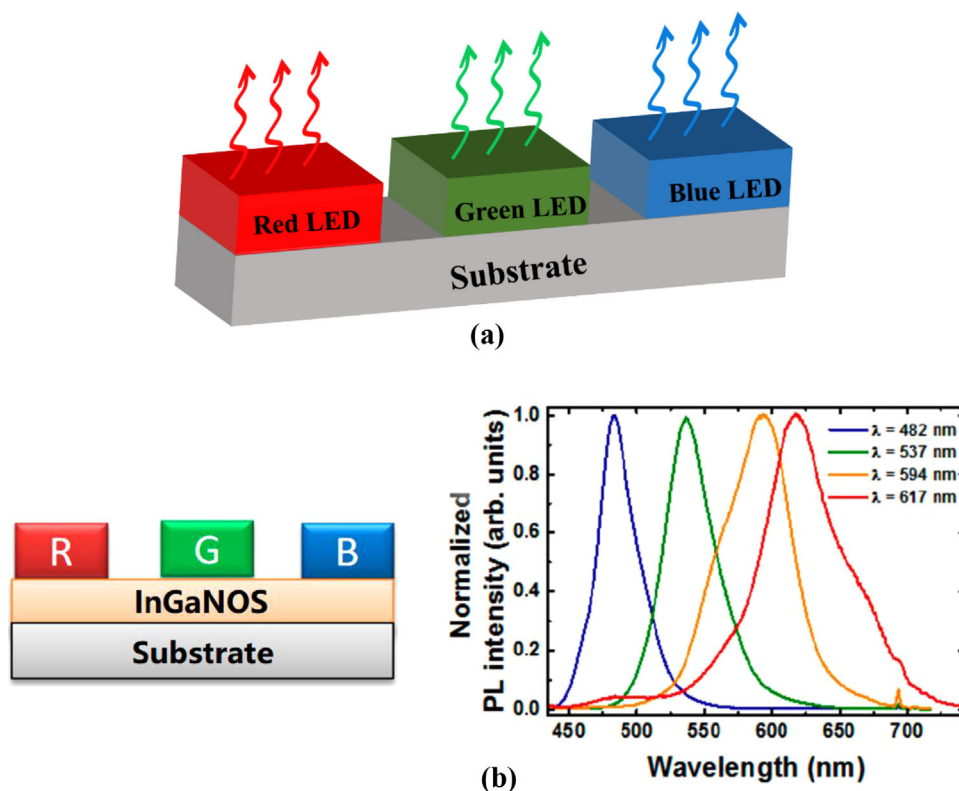
**ADVANCED
SCIENCE NEWS**

www.advancedsciencenews.com

LASER
& PHOTONICS
REVIEWS

www.lpr-journal.org

Figure 3. General mechanism of RGB-based micro-LEDs full color display. b) Illustration of InGaNOS substrate and PL spectra of InGaN-based LEDs grown on InGaNOS. Reproduced with permission.[1] Copyright 2018, MDPI publishing.

the bandgap decreases with increasing the QW width, which then leads to the redshift in light emission. However, this effect decreases the probability of the interband optical transitions and leads to lower EQE due to reduced electron–hole wave function overlap.[116,117] Additionally, the QCSE decreases with increasing the injection current due to the screening of the built-in electric field by free carrier.[118] The other option is to use the GaP/GaAs-based LEDs for red-light emission.[119] However, the difference in LEDs material (InGaN/GaN for blue and green while GaP/GaAs for the red color) leads to a difference in perspective of their key parameters (current, voltage, temperature, and device lifetime).[61,120] Consequently, the performance of the RGB display can be affected. Therefore, for the perfect realization of micro-LED-based RGB display, the same material system is required for all three primary colors.[121,122] To address this (red InGaN LEDs) challenge, different solutions including customized substrates, bandgap engineering, and optimized growth conditions have been reported.[123] For example, using the metamorphic InGaN buffer layers or InGaN pseudo-substrates (InGaNOS), which reduce the strain in InGaN QWs can lead to more efficient indium incorporation and better material quality for the active layer of LEDs.[124,125] Application of InGaNOS also leads to the enhancement of the spontaneous light emission and the EQE due to a reduction in the QCSE.[126–128] As a result, efficient light emission in the spectral range from 482 to 617 nm was achieved in InGaN-based LEDs grown on InGaNOS (as shown in **Figure 3**b).[1,128] More recently, porous GaN pseudo-substrates have been developed and red InGaN

micro-LEDs emitting at 632 nm have been demonstrated.[129,130] Further progress in InGaN pseudo-substrates will move the emission wavelength of InGaN LEDs to the IR spectral region.[131] Indium-rich InGaN pseudo-substrates can be used to decrease the energy gap of InN/InGaN QWs and QDs, moving further the emission spectrum to long wavelengths suitable for optical fiber communication.[132–134] In future perspectives, one can expect that InGaN pseudo-substrates will make it possible to reach the terahertz emission from InN/InGaN QWs and close the energy gap in these heterostructures, leading to the topological phase transition.[135] The theoretically proposed possibility of achieving the topological insulator state in InN-based QWs is currently of significant scientific interest due to their potential applications in piezotronics, spintronics, and topological electronics (topotronics)[136–142]

4.1. Color Conversion Method

The excitation source (blue/UV micro-LED) and color converters (phosphors/quantum dots) are required for full color display. The red, green, and blue color converters are needed with an excitation source of UV micro-LED, whereas only red and green color converters are required with blue micro-LED. However, the perfect deposition of color-converter on LED pixels is a challenge. Therefore, different printing technologies such as aerosol jet, inkjet, stamp, and coating techniques such as spin-coating, pulse spray, and mist have been attempted for the deposition of color-
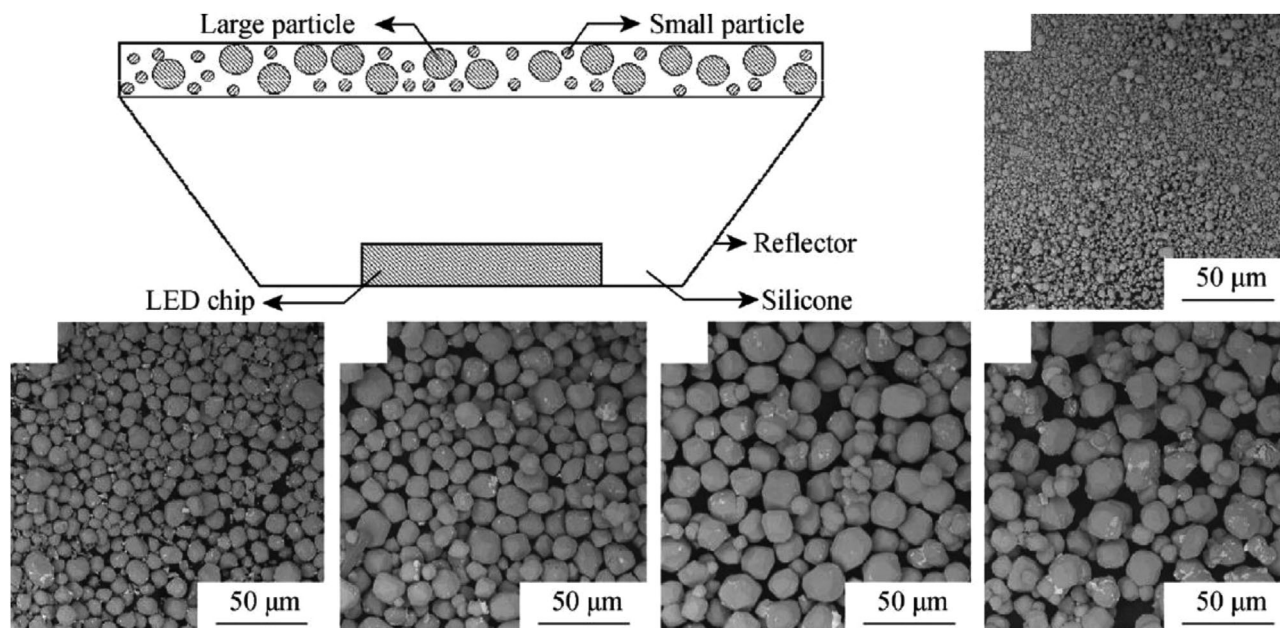
Figure 4. SEM images of phosphor with various mean particle diameter ranging from 4 to 26 µm. Reproduced with permission.[148] Copyright 2014, The Nonferrous Metals Society of China and Springer-Verlag Berlin Heidelberg.

converters.[143–146] Among them, the aerosol jet printing is better because it did not require contact and mask, give a very precise deposition, and is easy to handle with viscous ink.

4.1.1. Phosphor-Based Color Conversion

The prominent features of phosphors-based conversion technology are i) high quantum yield which is approximately more than 80%, ii) high thermal stability which is approximately above 150 °C, iii) high resistivity for the moisture (chemically stable), iv) fast-luminesce decay and very stable emission spectrum under the irradiation of continuous light flux. Because of these features, it is widely used to generate white light for lighting applications.[147–150] Normally, $Ca_{1-x}Sr_xS:Eu^{2+}$, $Sr_2Si_5N_8:Eu^{2+}$, $CaSiN_2:Ce^{3+}$ are used for generating a phosphor-based red emission, while, $SrGa_2S_4:Eu^{2+}$, $SrSi_2O_2N_2:Eu^{2+}$ for green light, and $LiCaPO_4:Eu^{2+}$, $Sr_5(PO_4)_3Cl:Eu^{2+}$ for blue light.[150] Another way of conversion is also possible in which phosphor-based conversion from blue micro-LED to white light is carried out, then color filters are used for full-color display. In this technology, a portion of the light is absorbed by the color-conversion filters which then lead to crosstalk among the sub-pixels because of the light scattering. Hence, an alternative and efficient way of conversion is required. Therefore, different deposition techniques have been explored to coat the phosphor layer on each pixel.[151,152]

For the successful realization of micro-LEDs-based full color display using phosphor as a color-conversion layer, the particle size of the phosphor is very important. The size of phosphor particles depends upon their preparation methodology, e.g., the solid-state reaction method normally leads to the particle size of greater than 5 µm, spray method to 100 nm to 2 µm, combustion to 500 nm to 2 µm, hydrothermal to 10 nm to 1 µm, sol–gel to 10 nm to 2 µm, and co-precipitation gives particle size of

10 nm to 1 µm.[147] This means that phosphor particles within the nanosize range can be achieved using the above technologies which will be useful for color uniformity. But on the other side, the light-conversion efficiency will be reduced[150] because light-conversion efficiency is inversely proportional to the size.

In order to overcome this trade-off between the light efficiency and color uniformity, Chen et al. have introduced small (4 µm) and large-sized (22 µm) phosphors particles together with the ratio of 3:2 in color-conversion layer[148] (**Figure 4**). In Summary, color uniformity can be enhanced by a phosphor-based color conversion layer with small (nano)-sized particles because of reduced light scattering. However, the use of these (nano)-sized particles in color conversion layer effectively reduces the light conversion efficiency and affects the performance of micro-LEDs-based full-color display. Therefore, it is required to explore other conversion materials to replace phosphor-based materials. With the prominent features of small-size and high light conversion efficiency, the QDs are promising candidates for future display applications.

4.1.2. QD-Based Color Conversion

QDs are compound semiconductor nanomaterials which are mostly from III–V (InP), II–VI (CdSe), or I–III–VI (CuInS₂).[153,154] QDs are normally developed using a chemical solution-based method.[155] QDs are a better replacement of phosphor as a conversion layer because of their tunable optical properties, color purity (narrow emission), shorter emission lifetime, high quantum yield, and strong absorption in the visible region. The emission wavelength of QDs can be controlled by the dimension and composition of QD particles.[153,156,157] The promising and widely reported QD material is CdSe (with an energy bandgap of 1.73 eV) whose emission can be tuned in the visible region with the best light-emitting efficiency.

**ADVANCED
SCIENCE NEWS**

www.advancedsciencenews.com

LASER
& PHOTONICS
REVIEWS

www.lpr-journal.org

Table 2. Comparison of different patterning techniques for QD deposition[23].

Deposition technique	Pattern width	QD film thickness
Inkjet printing	250 nm	Several µm
Electron beam lithography	Several µm	≈10 nm
Photolithography	Several µm	Several µm

Table 3. Requirements for micro-LEDs in different applications[1].

Application	Panel size [in.]	PPI	Chip size [µm]
AR	0.5–1	450–2000	1–5
Smart watch	1–1.5	200–300	5–30
Mobile phone	4–6	300–800	30–50
Auto display	6–12	150–250	50–100
TV	32–100	40–80	50–80
Digital display	150–220	20–30	80–100

Approximately, the CdSe QD with a diameter of 2 nm can emit blue light, whereas 8 nm QD can emit red color. Similarly, CdTe (with an energy bandgap of 1.5 eV) can emit a deeper wavelength (≈827 nm).[154,158,159] Numerous advanced techniques have been proposed for the patterning QDs on micro-LEDs, e.g., photolithography,[160] electron-beam lithography (EBL),[161] jet printing,[143] and 3D printing.[162] To select the QD patterning methodology, the various parameters such as resolution, throughput, and defect tolerance of the desired application (display) should be kept in mind. For example, the 55 in. TV with 4K resolution consists of the 10 µm × 10 µm micro-LED chip. This chip consists of ≈3 µm RGB subpixels. For 8K resolution, the subpixel size is less than ≈3 µm. Therefore, by using the EBL technique, the size of QD patterns can be scaled down to sub µm which is enough for micro-LEDs.[23] Manfrinato et al. reported nm resolution patterning using EBL.[163] By photolithography, the size of QD patterns of ≈2–5 µm in width and ≈50 µm in thickness, was achieved.[160] While, by utilizing printing technology, Richner et al. achieved QDs with the size of ≈250 nm.[164] The comparison of the various patterning techniques is given in **Table 2.** Consequently, it is possible to utilize any of the above-mentioned techniques for the deposition of QDs for the LED with micrometer size. Nevertheless, each technique has its own limitations. For example, the transfer printing technique needs a template which is making the procedure more complicated and inkjet printing has its own problems such as coffee ring effect, nonuniform film thickness, and rough surface of printed film. Similarly, for the photolithography and EBL, QD films can be easily damaged which will directly impact the production cost.

Comparatively, so far, the printing technology can meet most of the market demands because the pixel sizes for display are still above micrometers. Therefore, from the perspective of simple and rapid fabrication steps, the printing technique should be mainstream in future industries.

The light from the excitation source (blue/UV LED) is guided with a light guide plate which is comprised of a diffuser/distributed Bragg reflector (DBR) for uniform distribution of light across the display area. Then, this light is converted into primary colors (RGB) with a wide color gamut after passing through color-conversion layer. Three geometries are normally used for the deposition of QD color conversion material (shown in **Figure 5**a). i) On-chip: in this geometry, QD is deposited on LED, ii) On the edge: in which QD material is deposited at the edge of the light guided plate, and iii) On the surface: in which thin layer of QD is placed on the whole surface of the light guided plate which is called quantum dot enhanced film (QDEF).[17,165,166]

On the applications side, the requirement of micro-LEDs varies according to chip size, panel size, and pixel per inch (PPI). The details of a few applications are given in **Table 3.**

For the color conversion, the MQW structure (from the II–VI and III–V group) can also be used with micro-LED.[167] In 2015, Santos et al. showed the color conversion by MQW structure where they used 450 nm micro-LED to excite
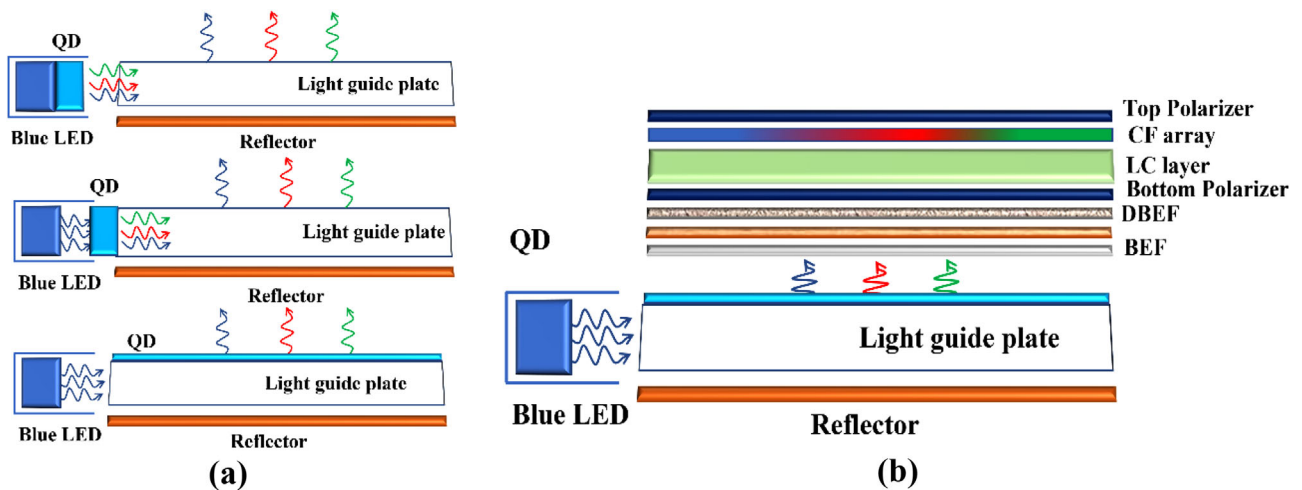

Figure 5. a) Schematic diagram of the various geometries of QD color converters: on-chip (top), on edge (middle), and on the surface (bottom). b) A typical LCD system with QDEF (QD on the surface of the light guided plate).
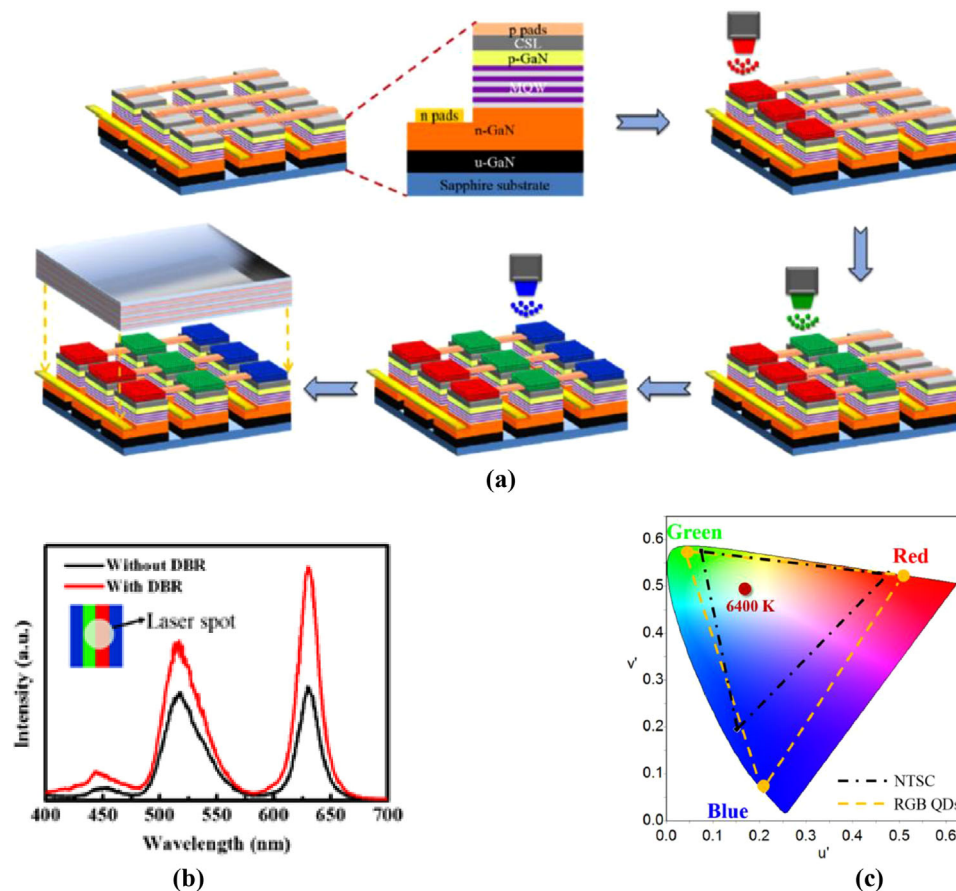
Figure 6. a) Flow process of full color QD-based μ-LED display. b) Comparison of relative PL intensity with and without DBR. c) The CIE 1976 color space chromaticity diagram of the QD display technology and NTSC. Reproduced with permission.[143] Copyright 2015, Optical Society of America.

ZnCdSe/ZnCdMgSe MQW structure to successfully realize a hybrid micro-LED emitting 540 nm light.[168]

In the beginning, Han et al. have reported the RGB QD-based micro-LED display using UV-LED (with 395 nm emission and chip size of 35 μm × 35 μm) as an excitation source.[143] Aerosol spray technology was used for the deposition of RGB QDs on top of the excitation source. The deposition was completed in three major steps; first pouring out the specific volume of QD particles which was regulated by applied voltage/gas pressure, then placing the QD particle at the required position, and finally spreading and drying it over the surface. The structural geometry of the proposed structure is shown in **Figure 6**a. DBR was used for the efficient utilization of UV light for light conversion which improved the luminous efficiency of blue by ≈194%, green by ≈173%, and red light by ≈183% (the relative PL intensity with and without DBR is also shown in Figure 6b). Moreover, the color gamut was 1.52 times of the standard NTSC gamut (shown in Figure 6c). However, the problem of optical crosstalk was there which needs to be addressed.

In 2017, Lin et al. have presented an idea to decrease the optical crosstalk by introducing a photoresist (PR) window which was prepared using lithographic technique.[169] This PR window acts as a light blocking wall from one pixel to another as shown in **Figure 7**a. Consequently, the optical crosstalk was significantly reduced in comparison to the conventional structure (without PR window) which is evident from Figure 7b. Moreover, they have used DBR to utilize the wasted light. As a result of both PR window and DBR, the light emission efficiency of QD was improved by ≈23%, ≈32%, and ≈5% for red, green, and blue light, respectively.

Gou et al. simulated micro-LED-based display structures by introducing funnel tube arrangement.[170] With the use of a funnel tube, the phosphor remains blocked in each pixel because it is deposited on a top surface of the LED with the tube area in a straight line to each sub-pixel. The internal region of the tube can be absorptive/reflective. For white light conversion, the phosphor was placed inside the tube. On the top surface, the RGB color filters were employed to separate the different colors. The schematic diagram of the arrangement is shown in Figure 7c. Consequently, the crosstalk was found to be effectively reduced in this arrangement.

In addition to crosstalk, the coffee ring is another problem that affects the uniform luminescence efficiency of QD-based micro display.[171] This is due to the formation of ring-shaped patterns at the edges. This problem is induced because of the differential rate of evaporation among the corner and inside of the QD droplet. This should be addressed to improve the uniform thickness of the QD color conversion layer.

The problem of the coffee ring can be solved by controlling the concentration of QD particles, dwell time and flow rate of gas,
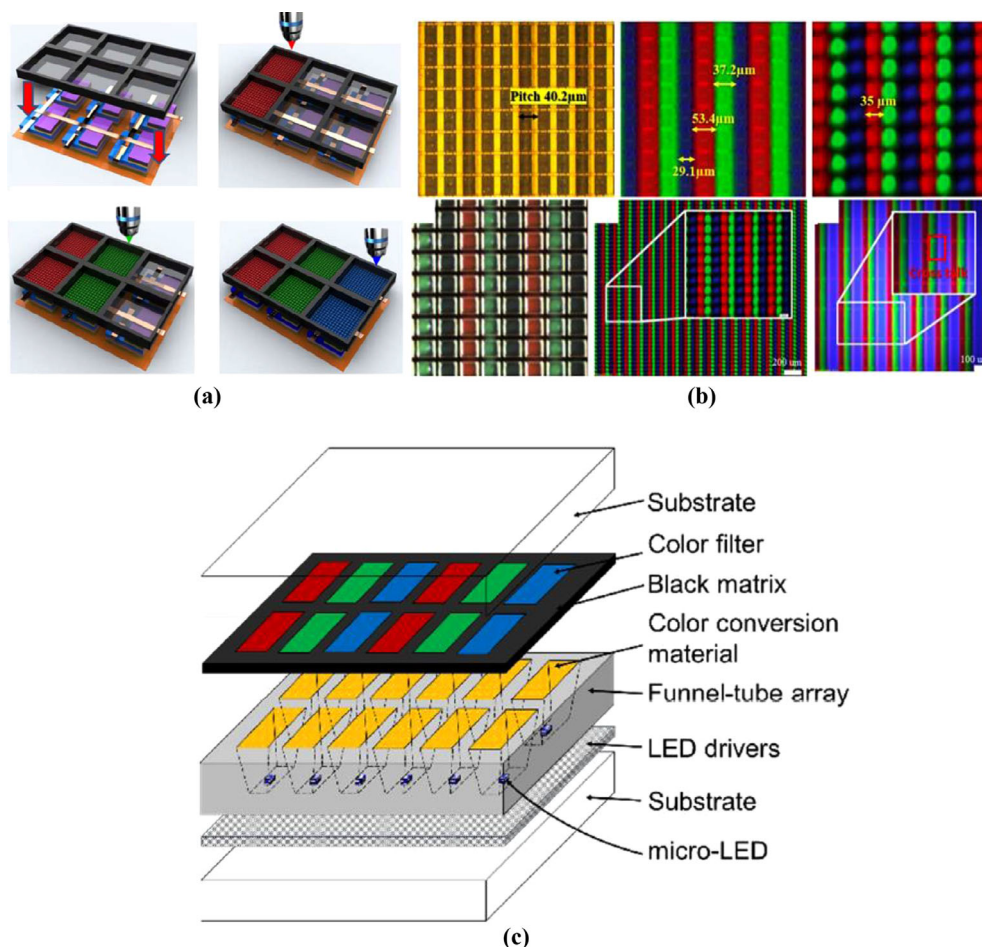
Figure 7. a) The flow process used for the reduction of optical cross talk in the full color micro-LED display. b) Microscopic images showing the comparison of effect of PR mold on optical cross talk. Reproduced with permission.[169] Copyright 2017, Chinese Laser Press. C) Schematic diagram of full color micro-LED display with funnel tube array. Reproduced with permission.[170] Copyright 2019, MDPI publishing.
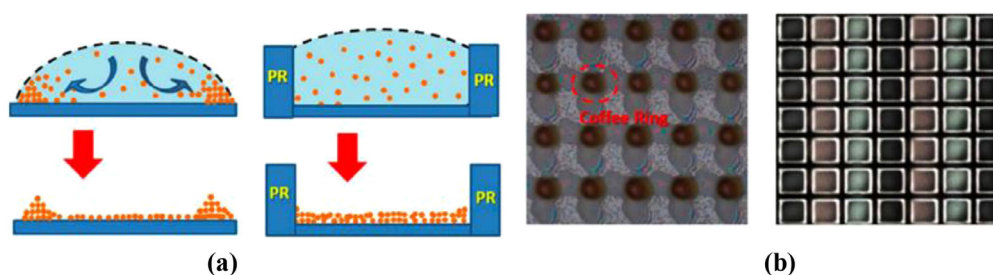

Figure 8. a) Mechanism of coffee ring effect (deposition at edges during evaporation) with/without PR mold. b) Comparison of the optical microscopic image with or without PR mold. Reproduced with permission.[169] Copyright 2017, Chinese Laser Press.

applied voltage, and size of the QD ejecting nozzle. The PR window, which was applied for the reduction of the optical crosstalk window, is also effective for minimizing the ring effect. By applying a resistant window, the QD solution within each window can be made uniform. **Figure 8** shows the comparison of both cases with or without PR window. The coffee ring-shaped effect was also addressed by the addition of polymers (hydro-soluble) where the enhancement in viscosity and Marangoni effect was observed.[171,172] There are also some other reports where the

problem of the coffee ring-shape effect was addressed, e.g., Liu et al. controlled some of the key parameters, namely, viscosity, three-phase contact line, and contact angle, by using a composite of QD ink. Consequently, they obtained a QD film with uniform thickness. Similarly, Sun et al. improved the viscosity, surface tension, and evaporation rate of perovskite ($CsPbBr_3$)-based QD ink by changing the volume of dodecane and toluene (solvents) to form suitable Marangoni flow. As a result, they obtained uniform perovskite microarrays.[173,174]
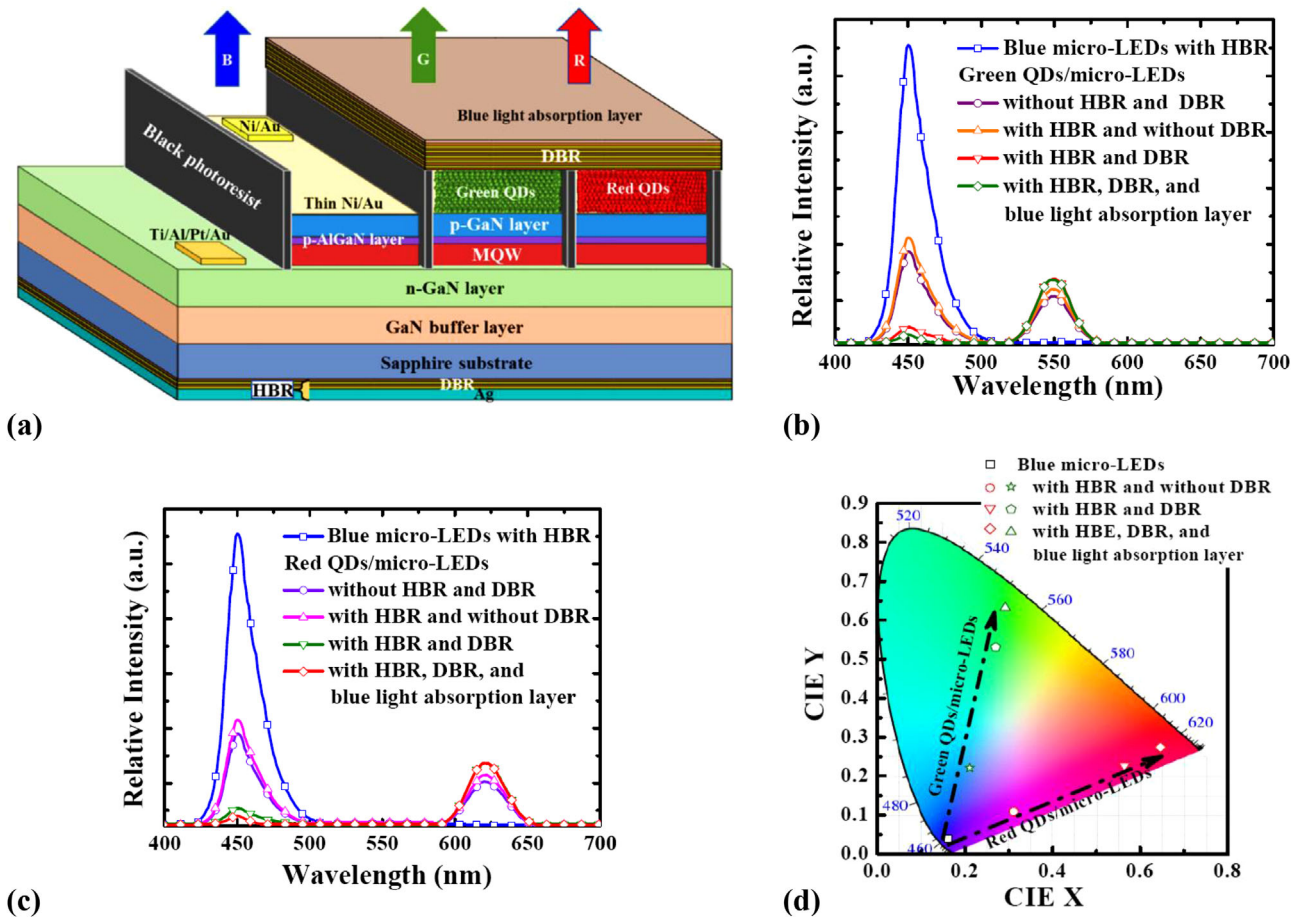
**ADVANCED
SCIENCE NEWS**

www.advancedsciencenews.com

LASER
& PHOTONICS
REVIEWS

www.lpr-journal.org

Figure 9. a) Schematic diagram of RGB micro-LED with HBR and DBR. b,c) EL spectra of green and red QD-based micro-LEDs. d) International commission on illumination (CIE) chromaticity coordinates of device structures with and without HBR and DBR. Reproduced with permission.[179] Copyright 2020, MDPI publishing.

Another problematic issue in the QD-based micro-LED display is the leakage of blue light from the excitation source. Different strategies such as DBF or color-conversion filter (consisting of primary colors: RGB) has been used to solve this problem.[169,175] However, both DBF and color-conversion filters led to the fabrication complexity and also increases the overall cost of fabrication. The problem of blue light leakage can be also solved through the easiest approach, e.g., by using the different concentrations of the QDs. In the reported literature, the relation between the absorption and concentration of QDs is represented by the below equation (which is also called Beer's law)[176]

$$A = \varepsilon \times C \times t = \log\left(\frac{I_{in}}{I_{out}}\right) \tag{1}$$

where A is the absorption coefficient, ε is the extinction coefficient, C is the concentration of QD, and t is the length of the optical path. It has been reported that the green and red QD film with a thickness of ≈5 μm can absorb nearly 99% of blue light.[177] Similarly, Lee et al. have fabricated ≈10 μm thick InP/ZnS QD film using inkjet-printing technique[178] to achieve >95% absorption of blue light. Their film showed good stability under high humidity (i.e., 95% relative humidity) and temperature (65 °C).

There are many reports about the performance up-gradation of the micro-LED display, e.g., Chu et al. have reported the micro-LED-based RGB display using CdSe/ZnS QDs as color conversion materials and GaN-based blue micro-LEDs as excitation sources.[179] To improve the color contrast ratio, they confined each QD light using a black matrix (which have the property of nearly no transmission in the visible region) as shown in **Figure 9**a. The hybrid Bragg reflector (HBR) and DBR were deposited on the back and top side, respectively, to improve the reflection of light from the substrate side and also the color purity. As a result, the light output intensities and the color purity of both green and red QDs were improved (Figure 9b–d). In the traditional design of a QD-based micro-LED display, the QD layer is deposited on the top of the encapsulation layer. In this architecture, the portion of the light was trapped between the encapsulation and QD layer because of the total internal reflection. As a result, the radiative coupling between the MQW and QDs was reduced which directly impacted the efficiency of the display. In order to improve the radiative coupling efficiency, various strategies have been reported, e.g., surface roughening of LEDs and etched nanostructures like photonic crystals have been used.[180,181] Normally, these strategies are only effective for the top layer (quantum barrier).
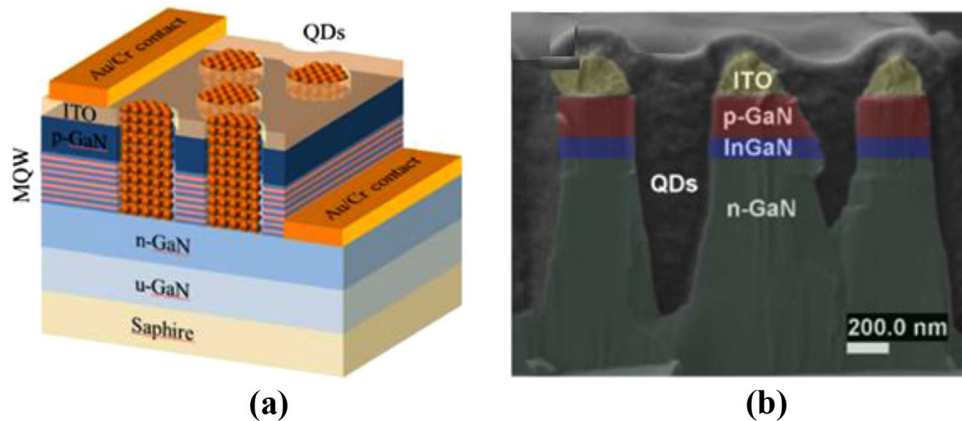
Figure 10. a) Systematic diagram of photonic quasi-crystal LED hybridized with QD color converter. b) SEM image of cross-sectional area. Reproduced with permission.[182] Copyright 2016, Optical Society of America.

Krishnan et al. developed a hybrid photonic quasi-crystal LED to increase the radiative coupling between MQWs and QDs. In this device geometry, the QD emitters were placed in proximity to the active region (**Figure 10**).[182] As a result, the color-conversion quantum yield of a single QD (monochromatic conversion) was enhanced by ≈123% and for QD-based white display, it was increased by ≈110%. From color conversion efficiency (CCE) formula, energy transfer from MQW (active region) to QD via both radiative and nonradiative (resonant energy transfer) pathways can be estimated. The CCE is expressed as a ratio of the light emission intensity of QDs (from the hybridized structure) to the light emission intensity from MQWs without QDs.[183] Mathematically it can be expressed as

$$\text{CCE} = \frac{\int I_{\text{QDs}}^{\text{Hybrid}}(\lambda)\, d\lambda}{\int I_{\text{MQW}}^{\text{no QDs}}(\lambda)\, d\lambda} \tag{2}$$

here the wavelength of the emitted light is denoted by λ. Moreover, the efficiency of color conversion, i.e., effective quantum yield (EQY) can be estimated by taking the ratio of photons emitted at QD wavelength (from the hybrid structure) to the quenched photons which are emitted at MQW wavelength (after the hybridization of structure)

$$\text{EQY} = \frac{\int I_{\text{QDs}}^{\text{Hybrid}}(\lambda)\, d\lambda}{\int I_{\text{MQW}}^{\text{no QDs}}(\lambda)\, d\lambda - \int I_{\text{QDs}}^{\text{Hybrid}}(\lambda)\, d\lambda} \tag{3}$$

In the above formula, the denominator shows the difference in luminescence intensity with (emission from MQW) and without QDs (hybrid structure).

In micro-LED displays, the CCE can be enhanced by Förster resonant energy transfer (FRET).[184–186] In 2017, Wang et al. have proposed a nanoring (NR) structure instead of nanoholes/nanorod structures to enhance FRET (shown in **Figure 11**a).[187] In both nanoholes/nanorod structures, only one sidewall either inner or outer is contacted with QDs. Albeit, in NR structure, there is a probability of both sidewalls to contact with QDs, which can effectively enhance the CCE. They fabricated NR-LEDs with different sidewall widths ranging from 40

to 120 nm using nanosphere lithography. With the reduction in width, the induced strain within the active region because of lattice mismatch was relaxed. This was confirmed by photoluminescence (PL) and time-resolved PL measurements. Further, they observed a considerable blue shift (from green to blue) and the magnitude of this shifting increased with the decrease in sidewall thickness (Figure 11b). Hence, this (NR) can be a promising structure for the realization of nanometer-scale RGB LEDs for display applications. In 2019, Chen et al. proposed a feasible route for RGB micro-LEDs display using NR structure.[188] They have fabricated NR onto the micro-LED wafer (having emission in green regime), then by using the concept of strain relaxation with a blue shift, the emission wavelength was tuned from green to blue. Moreover, the PL intensity was enhanced by ≈143%, with the deposition of Al_2O_3 (passivation layer) within the sidewall of NR micro-LEDs.[66] Finally, red QDs were deposited on NR-LED. As shown in Figure 11c, without passivation layer, they achieved nonradiative resonant energy transfer (NRET) of ≈53% and with the passivation layer, NRET of ≈66% in QD-based NR micro-LED. NRET has a very important role because it is strongly correlated with the lifetime of exciton recombination.[189] Hence, they have presented a strategy for display with a wider color gamut (which overlap with ≈104% of the National television standards committee (NTSC) & ≈78% Rec. 2020) as shown in Figure 11e.

The light absorption and emission property of QDs also need to be improved because the dried films of QD suffered from serious challenges of color purity and lower quantum yield (QY), and are also hard to pattern with stable structure.[190,191] Therefore, it is required to add dried QD film with polymers/passivation layers to improve light absorption and emission property.[192–194]

Kang et al. introduced a nanoporous (NP) GaN to improve the light absorption as shown in **Figure 12**a.[195] They varied porosities (25%, 55%, and 75%) of NP GaN and studied its effect on light scattering and transport mean free path (TMFP). Normally, short TMFP is better because it allows multiple light scattering which increases its travelling path. The diffusion equation was used to estimate their light scattering and TMFP. In simple words, it can be expressed as the average distance, i.e., the distance in which light propagation is randomized completely and extracted from the measured value of transmittance.[197–200] The
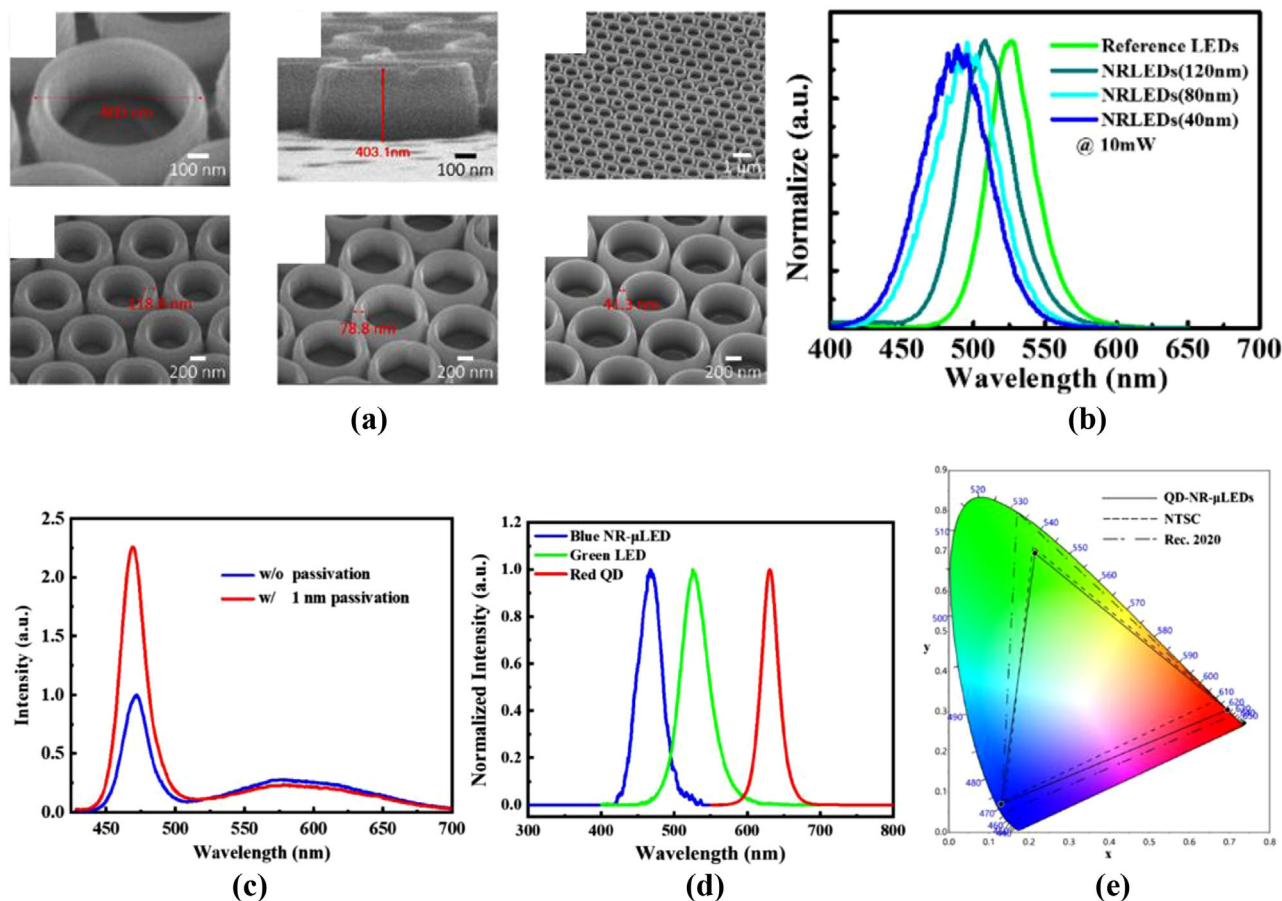
**ADVANCED
SCIENCE NEWS**

www.advancedsciencenews.com

**LASER
& PHOTONICS
REVIEWS**

www.lpr-journal.org

Figure 11. a) SEM images of NR LEDs with different wall widths (120, 80, and 40 nm). b) PL spectra with an excitation power of 10 mW. Reproduced with permission.[187] Copyright 2017, The Authors, published by Springer Nature. c) PL spectra of NR-LEDs with and without ALD passivation layer. d) EL spectra of RGB hybrid QD-based NR micro-LED. e) Color gamut of RGB hybrid QD-based NR micro-LED, NTSC and Rec. 2020. Reproduced with permission.[188] Copyright 2019, Chinese Laser Press.

TMFP can be evaluated using the mathematical expression given below

$$T_d = \frac{(1 + z_e) - \left[1 + z_e + \frac{L}{l^*}\right] e^{\left[\frac{-L}{l_s}\right]}}{\left(\frac{L}{l^*}\right) + 2z_e} \tag{4}$$

where T_d, z_e, L, and l_s is diffusion transmittance, extrapolation length, total thickness of medium (scattering medium), and mean free length of scattering path, respectively. The detail is provided in refs. [197,201] In NP GaN with 75% porosity, the light extinction coefficient was increased by 11 times at 370 nm due to multiple scattering. As a result, the light CCE of green and red light was enhanced by 96% and 100%, respectively (Figure 12b). Kang and Han also reported another strategic way where they employed the QDs into NP-GaN which is composed of both vertical and horizontal nanopores (scanning electron microscope (SEM) images are shown in Figure 12d).[196] The probability of light absorbance of QD (on NP GaN) was much higher than the planar surface (non-NP GaN) due to the increase in length of the optical light path. The nanopores can effectively scatter the light in

the perpendicular direction.[202] But in this structure (with both vertical and horizontal nanopores), at a low incident angle, most portion of the light was scattered by the horizontal nanopores. Therefore, this structure is more promising for attaining efficient light conversion.

Recently, in 2020, Mei et al. have introduced a facile route, i.e., sacrificial layer-assisted patterning (SLAP) approach in comparison to previously photolithographic techniques for the fabrication of QD-based LEDs display.[203] In photolithographic technique, both the device performance and purity of emission color are severely suffered. However, in SLAP, the presence of a sacrificial layer (SL) enhances the contact and stability of QDs. They used both negative PR layer and SL for the deposition of QDs (**Figure 13**a) and reported 500 pixels per inch prototype of full-color QD-based LED. Using SLAP, they improved the color purities of the light and achieved a wider color gamut which is ≈114% of NTSC (Figure 11). This methodology can be applied for the mass production of a high-resolution display with reduced cost. Almost, to date, this is the first report of a high-resolution (500 ppi) full-color QD-based LED display.

In the photolithography process, the problem to fabricate full-color display (QD-based LED) mainly comes from the interface
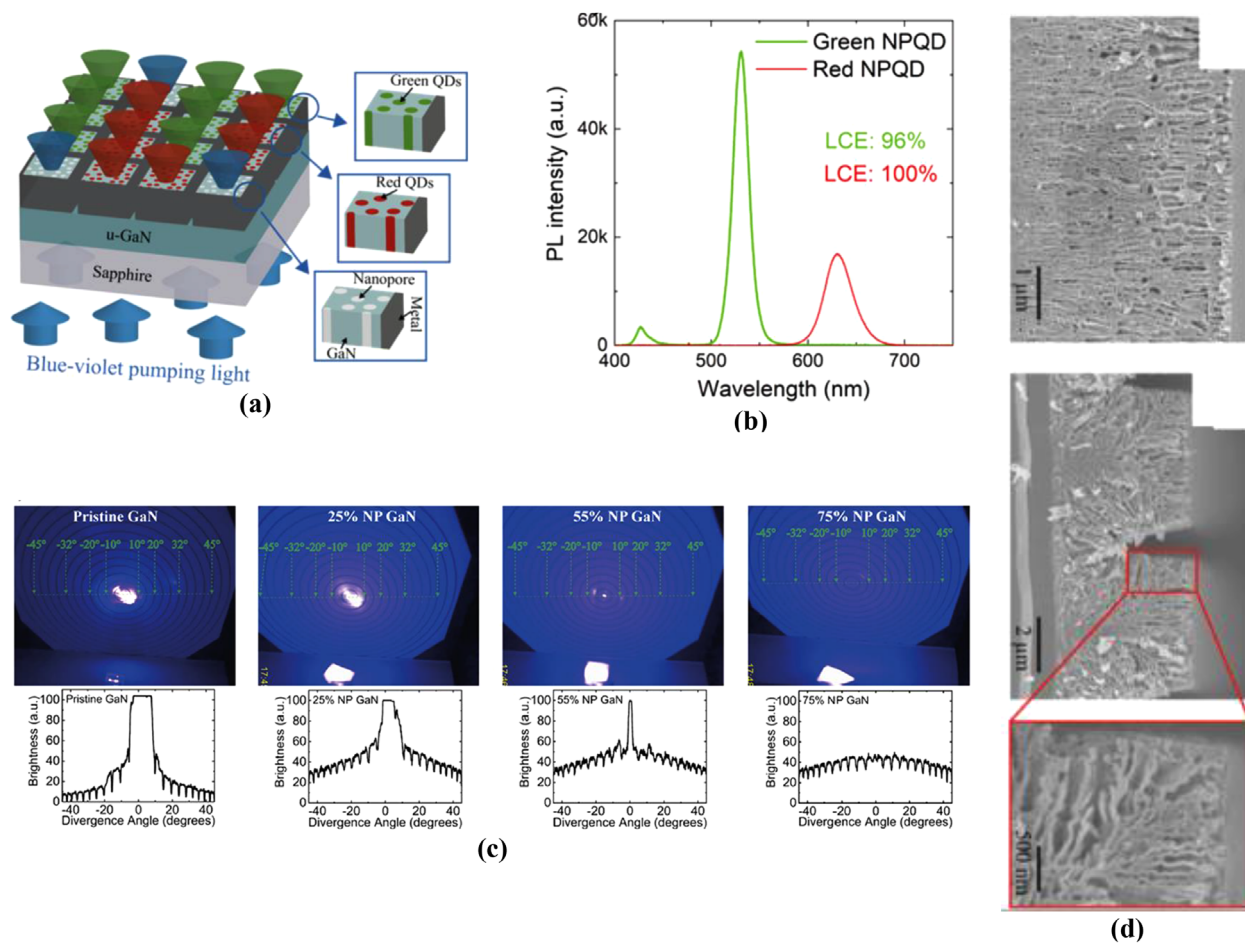
**ADVANCED
SCIENCE NEWS**

www.advancedsciencenews.com

LASER
& PHOTONICS
REVIEWS

www.lpr-journal.org

Figure 12. a) Schematic diagram of QD-based micro-LED (NP GaN embedded with QDs). b) PL spectra of green and red NP QD LED. c) Visualization of light scattering by pristine GaN and NP GaN. Reproduced with permission.[195] Copyright 2020, American Chemical Society. d) Cross-sectional SEM images of vertical and hybrid NP GaN electrochemically etched at 22 V. Reproduced with permission.[196] Copyright 2019, The Society for Information Display.

(QD/substrate or QD/PR interface) in direct approaches. Because interfaces require both materials with the same characteristics. In SLAP (indirect approach), the problem is PR/sacrificial layer (SL) which can be solved through careful selection of the SL material. The SL materials are not necessary to be photo-responsive. This SLAP technology can be combined with various other patterning technologies, i.e., photolithography, transfer printing, laser writing, and so on to attain easy QD patterning. Hence, this innovative patterning technique will open a new horizon for future display technologies and may lead to a nondisruptive and innovative change in the display industry.

5. Conclusion and Future Directions

This article reviewed the recent development of display technologies ranging from LCD to RGB full-color LED-based display. Almost, from the beginning of the 21th century, high-performance displays are kept playing a key role from the generation of internet-enabled computers, to smartphones and present IoT (Internet of Things) devices. To meet the desired demand of the market, cost-effective, efficient, and environmental-friendly smart display products with high picture quality are needed. Several emerging technologies have been developed to replace the traditional technologies of LCD, OLEDs, and micro-LEDs. Among the traditional technologies, OLED-based products have been successfully commercialized and are mostly being used in mobile phone displays. Albeit, it is hard to attain high resolution (more than 600 ppi) using evaporation/inkjet printing techniques. On the other side, micro-LEDs have an exceptionally high manufacturing cost because of their low yield of chip transfer. Further, their efficiency is greatly degraded by decreasing their dimension from LED to micro-LED. We reviewed several technologies with remedies to overcome their negative impact on the realization of full-color display. Integration of various colors emitting micro-LEDs and materials on the same substrate through mass transfer and bonding is the main pathway for future RGB full-color micro-LED display. Therefore, we compare various mass transfer technologies in terms of their performance rate. Overall, it is needed to improve the yield of mass transfer with a decrease in its cost. Besides mass transfer technology, the other option is color conversion technology where there is no need for a separate wafer for each color. Only an excitation source (i.e., blue/
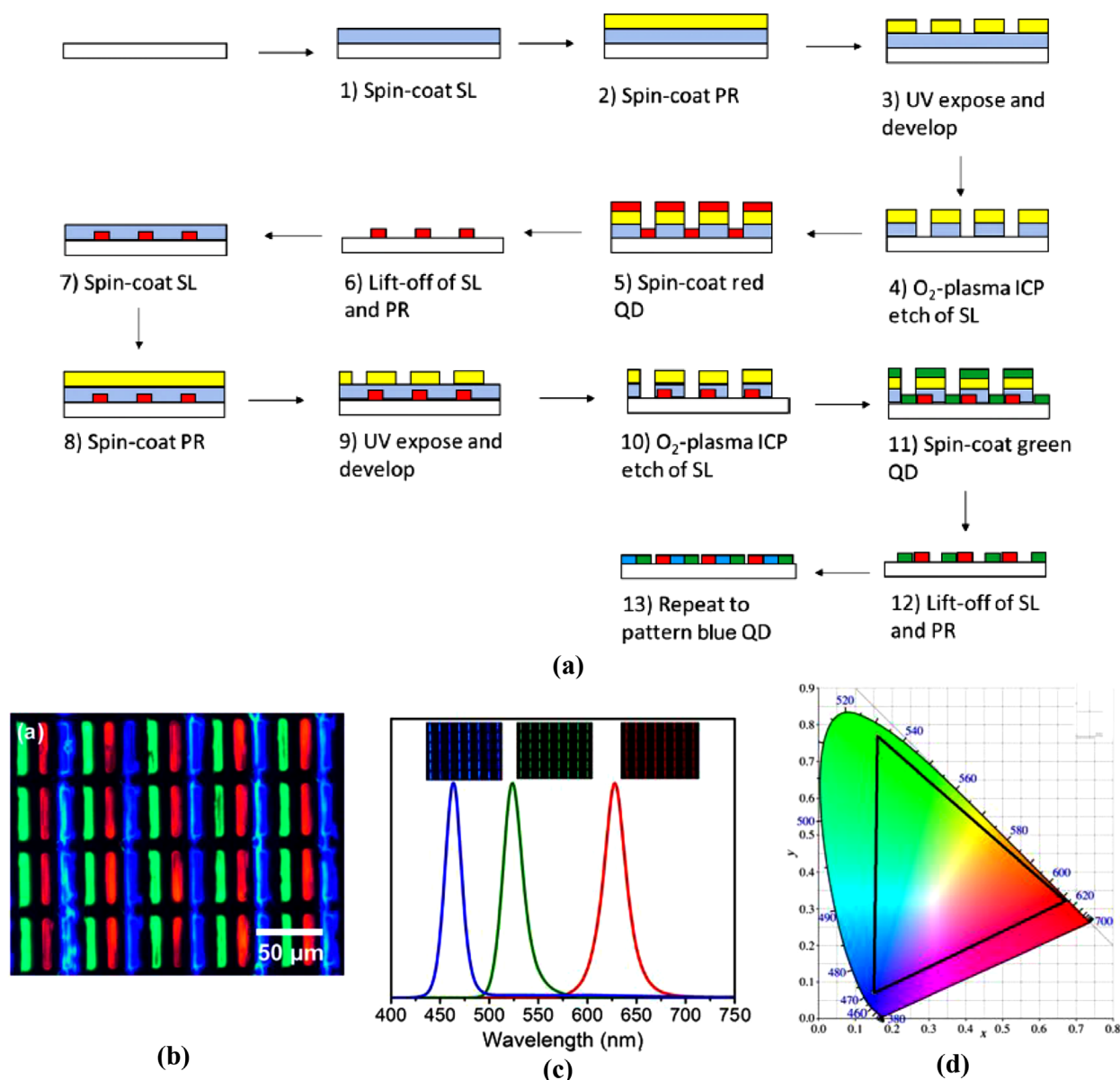
**ADVANCED
SCIENCE NEWS**

www.advancedsciencenews.com

LASER
& PHOTONICS
REVIEWS

www.lpr-journal.org

Figure 13. a) Illustration of patterning QDs with different color via photolithographic technique. b) PL image of patterned RGB QDs. c) Emission spectra and d) color gamut of RGB subpixels. Reproduced with permission.[203] Copyright 2020, American Chemical Society.

UV) and color conversion layers for multi-color (RGB) emission are needed. QDs are the most prominent medium for color conversion and their deposition methodology is relatively mature. Albeit, their CCE is not best and decreased under the light. In this review article, we discussed the key features required for QD-based color conversion including I) structural geometries for the deposition of QDs, II) utilization of DBR and HBR, III) PR layer to minimize the optical cross-talk and also to reduce the coffee rings effect, IV) structures (nanorings, nanorods, and nanoholes) for efficient light coupling from the active region to QDs, and V) the development of new methodology (SLAP) compared to simple photolithography. In the nutshell, various strategical reports are reviewed for achieving the best solution for RGB full-color display by LED integration. It is logical to predict breakthroughs

in upcoming years. Therefore, we believe that micro-LED will be used as future display technology because of its lifetime, low energy consumption, high resolution, and wider color gamut with high purity.

Acknowledgements

Conflict of Interest

The authors declare no conflict of interest.

Keywords

[1] T. Wu, C.-W. Sher, Y. Lin, C.-F. Lee, S. Liang, Y. Lu, et al., *Appl. Sci.* **2018**, *8*, 1557.

[2] J. Day, J. Li, D. Lie, C. Bradford, J. Lin, H. Jiang, *Proc. SPIE* **2012**, *8268*, 82681X.

[3] H.-S. Kim, E. Brueckner, J. Song, Y. Li, S. Kim, C. Lu, J. Sulkin, K. Choquette, Y. Huang, R. G. Nuzzo, J. A. Rogers, *Proc. Natl. Acad. Sci. U. S. A.* **2011**, *108*, 10072.

[4] H. J. Jang, J. Y. Lee, J. Kim, J. Kwak, J.-H. Park, *J. Inf. Disp.* **2020**, *21*, 1.

[5] L. Robert, A. Barbin, *Wiley Encyclopedia of Electrical and Electronics Engineering*, Wiley Online Library, Hoboken, NJ **1999**.

[6] N. Chang, I. Choi, H. Shim, *IEEE Trans. Very Large Scale Integr. (VLSI) Syst.* **2004**, *12*, 837.

[7] S. Kobayashi, S. Mikoshiba, S. Lim, *LCD Backlights*, vol. 21, John Wiley & Sons, New York **2009**.

[8] M. Schadt, *Jpn. J. Appl. Phys.* **2009**, *48*, 03B001.

[9] F. Peng, H. Chen, F. Gou, Y.-H. Lee, M. Wand, M.-C. Li, et al., *J. Appl. Phys.* **2017**, *121*, 023108.

[10] C.-H. Li, S.-H. Lu, S.-Y. Lin, T.-Y. Hsieh, K.-S. Wang, W.-H. Kuo, *SID Symp. Dig. Tech. Pap.* **2018**, *49*, 678.

[11] C. W. Tang, S. A. VanSlyke, *Appl. Phys. Lett.* **1987**, *51*, 913.

[12] B. Geffroy, P. L. Roy, C. Prat, *Polym. Int.* **2006**, *55*, 572.

[13] H. Chen, G. Tan, S.-T. Wu, *Opt. Express* **2017**, *25*, 33643.

[14] L. Ma, Y.-F. Shao, *J. Cent. South Univ.* **2020**, *27*, 1624.

[15] J.-H. Lee, C.-H. Chen, P.-H. Lee, H.-Y. Lin, M.-K. Leung, T.-L. Chiu, C.-F. Lin, *J. Mater. Chem. C* **2019**, *7*, 5874.

[16] E. L. Hsiang, Z. Yang, Q. Yang, Y. F. Lan, S. T. Wu, *J. Soc. Inf. Disp.* **2021**, *29*, 446.

[17] H.-W. Chen, J.-H. Lee, B.-Y. Lin, S. Chen, S.-T. Wu, *Light: Sci. Appl.* **2018**, *7*, 17168.

[18] H. Jiang, J. Lin, *Opt. Express* **2013**, *21*, A475.

[19] F. Olivier, A. Daami, L. Dupré, F. Henry, B. Aventurier, F. Templier, *SID Symp. Dig. Tech. Pap.* **2017**, *48*, 353.

[20] F. Templier, *J. Soc. Inf. Disp.* **2016**, *24*, 669.

[21] Y. Wu, J. Ma, P. Su, L. Zhang, B. Xia, *Nanomaterials* **2020**, *10*, 2482.

[22] R. Zhu, Z. Luo, H. Chen, Y. Dong, S.-T. Wu, *Opt. Express* **2015**, *23*, 23680.

[23] Z. Liu, C.-H. Lin, B.-R. Hyun, C.-W. Sher, Z. Lv, B. Luo, F. Jiang, T. Wu, C.-H. Ho, H.-C. Kuo, J.-H. He, *Light: Sci. Appl.* **2020**, *9*, 83.

[24] H. Choi, C. Jeon, M. Dawson, P. Edwards, R. Martin, S. Tripathy, *J. Appl. Phys.* **2003**, *93*, 5978.

[25] B. Thibeault, S. DenBaars, *US6410942B1*, **2002**.

[26] C. Bower, S. Bonafede, E. Radauscher, A. Pearson, B. Raymond, E. Vick, et al., *Proc. SPIE* **2020**, *11302*, 1130202.

[27] K. Ding, V. Avrutin, N. Izyumskaya, Ü. Özgür, H. Morkoç, *Appl. Sci.* **2019**, *9*, 1206.

[28] B.-R. Hyun, C.-W. Sher, Y.-W. Chang, Y. Lin, Z. Liu, H.-C. Kuo, *J. Phys. Chem. Lett.* **2021**, *12*, 6946.

[29] Y. Lin, X. Zheng, Z. Shangguan, G. Chen, W. Huang, W. Guo, et al., *J. Mater. Chem. C* **2021**, *9*, 12303.

[30] J. J. McKendry, R. P. Green, A. Kelly, Z. Gong, B. Guilhabert, D. Massoubre, et al., *IEEE Photonics Technol. Lett.* **2010**, *22*, 1346.

[31] X. Liu, P. Tian, Z. Wei, S. Yi, Y. Huang, X. Zhou, et al., *IEEE Photonics J.* **2017**, *9*, 7204909.

[32] D. Zhu, D. Wallis, C. Humphreys, *Rep. Prog. Phys.* **2013**, *76*, 106501.

[33] H. Ryu, K. Jeon, M. Kang, H. Yuh, Y. Choi, J. Lee, *Sci. Rep.* **2017**, *7*, 44814.

[34] J. Zhao, H. Hu, Y. Lei, H. Wan, L. Gong, S. Zhou, *Nanomaterials* **2019**, *9*, 1634.

[35] A. C. Cavazos Sepulveda, M. Diaz Cordero, A. A. A. Carreno, J. M. Nassar, M. M. Hussain, *Appl. Phys. Lett.* **2017**, *110*, 134103.

[36] W. Yang, K. Hu, F. Teng, J. Weng, Y. Zhang, X. Fang, *Nano Lett.* **2018**, *18*, 4697.

[37] A. Dadgar, *Phys. Status Solidi* **2015**, *252*, 1063.

[38] A. Gwyer, H. Phillips, *J. Inst. metals* **1926**, *36*, 283.

[39] A. Dadgar, in *III–V Compound Semiconductors: Integration with Silicon-Based Microelectronics* (Eds: T. Li, M. Mastro, A. Dagar), CRC Press, Boca Raton, FL **2010**, p. 137.

[40] A. Dadgar, A. Krost, *III-Nitride Semiconductors and their Modern Devices*, (Ed: B. Gil) Vol. 18, Oxford University Press, Oxford **2013**, p. 78.

[41] A. Dadgar, A. Alam, T. Riemann, J. Bläsing, A. Diez, M. Poschenrieder, et al., *Phys. Status Solidi* **2001**, *188*, 155.

[42] X. L. Nguyen, T. N. N. Nguyen, V. T. Chau, M. C. Dang, *Adv. Nat. Sci.: Nanosci. Nanotechnol.* **2010**, *1*, 025015.

[43] P. Schlotter, J. Baur, C. Hielscher, M. Kunzer, H. Obloh, R. Schmidt, et al., *Mater. Sci. Eng., B* **1999**, *59*, 390.

[44] G. Li, W. Wang, W. Yang, Y. Lin, H. Wang, Z. Lin, et al., *Rep. Prog. Phys.* **2016**, *79*, 056501.

[45] S.-M. Pan, R.-C. Tu, Y.-M. Fan, R.-C. Yeh, J.-T. Hsu, *IEEE Photonics Technol. Lett.* **2003**, *15*, 646.

[46] C. Hernández-Gutiérrez, Y. Casallas-Moreno, D. Cardona, Y. Kudriavtsev, A. Morales-Acevedo, G. Santana-Rodríguez, *IEEE 44th Photovoltaic Specialist Conf. (PVSC)*, IEEE, Piscataway, NJ **2017**, pp. 670–672.

[47] C. Chiu, P. Yu, C. Chang, C. Yang, M. Hsu, H. Kuo, et al., *Opt. Express* **2009**, *17*, 21250.

[48] C. Hernández-Gutiérrez, Y. Kudriavtsev, D. Cardona, A. Hernández, J. Camas-Anzueto, *Opt. Mater.* **2021**, *111*, 110541.

[49] F. Olivier, S. Tirano, L. Dupré, B. Aventurier, C. Largeron, F. Templier, *J. Lumin.* **2017**, *191*, 112.

[50] S. F. Chichibu, A. Uedono, T. Onuma, B. A. Haskell, A. Chakraborty, T. Koyama, et al., *Nat. Mater.* **2006**, *5*, 810.

[51] J.-J. Huang, H.-C. Kuo, S.-C. Shen, *Nitride Semiconductor Light-Emitting Diodes (LEDs): Materials, Technologies, Applications*, Woodhead Publishing, Sawston, UK **2017**.

[52] K. Lee, C.-R. Lee, T.-H. Chung, Y. S. Kim, K.-U. Jeong, J. S. Kim, *Opt. Express* **2016**, *24*, 24153.

[53] F. Lu, D. Lee, D. Byrnes, E. Armour, W. Quinn, *Sci. China: Technol. Sci.* **2011**, *54*, 33.

[54] H. Aida, D. S. Lee, M. Belousov, K. Sunakawa, *Jpn. J. Appl. Phys.* **2011**, *51*, 012102.

[55] M. Usman, A.-R. Anwar, M. Munsif, *ECS J. Solid State Sci. Technol.* **2020**, *9*, 066002.

[56] H. Aida, H. Takeda, N. Aota, K. Koyama, *Jpn. J. Appl. Phys.* **2011**, *51*, 016504.

[57] P. Tian, J. J. McKendry, Z. Gong, B. Guilhabert, I. M. Watson, E. Gu, et al., *Appl. Phys. Lett.* **2012**, *101*, 231110.

[58] T. Onuma, N. Sakai, T. Igaki, T. Yamaguchi, A. Yamaguchi, T. Honda, *J. Appl. Phys.* **2012**, *112*, 063509.

[59] K. A. Bulashevich, S. Y. Karpov, *Phys. Status Solidi RRL* **2016**, *10*, 480.

[60] P. Li, H. Li, H. Zhang, C. Lynsky, M. Iza, J. S. Speck, et al., *Appl. Phys. Lett.* **2021**, *119*, 081102.

[61] D. Hwang, A. Mughal, C. D. Pynn, S. Nakamura, S. P. DenBaars, *Appl. Phys. Express* **2017**, *10*, 032101.

[62] S. Usami, Y. Ando, A. Tanaka, K. Nagamatsu, M. Deki, M. Kushimoto, et al., *Appl. Phys. Lett.* **2018**, *112*, 182106.

[63] X. Zhou, P. Tian, C.-W. Sher, J. Wu, H. Liu, R. Liu, et al., *Prog. Quantum Electron.* **2020**, *71*, 100263.

[64] Y. Huang, E.-L. Hsiang, M.-Y. Deng, S.-T. Wu, *Light: Sci. Appl.* **2020**, *9*, 105.

[65] W. Chen, G. Hu, J. Lin, J. Jiang, M. Liu, Y. Yang, et al., *Appl. Phys. Express* **2015**, *8*, 032102.

[66] M. S. Wong, D. Hwang, A. I. Alhassan, C. Lee, R. Ley, S. Nakamura, et al., *Opt. Express* **2018**, *26*, 21324.

[67] L. Zhang, F. Ou, W. C. Chong, Y. Chen, Q. Li, *J. Soc. Inf. Disp.* **2018**, *26*, 137.

[68] R. S. Cok, M. Meitl, R. Rotzoll, G. Melnik, A. Fecioru, A. J. Trindade, et al., *J. Soc. Inf. Disp.* **2017**, *25*, 589.

[69] B. Corbett, R. Loi, W. Zhou, D. Liu, Z. Ma, *Prog. Quantum Electron.* **2017**, *52*, 1.

[70] E. H. Virey, N. Baron, Z. Bouhamri, *SID Symp. Dig. Tech. Pap.* **2019**, *50*, 129.

[71] J. Li, B. Luo, Z. Liu, *21st Int. Conf. Electronic Packaging Technology (ICEPT)*, IEEE, Piscataway, NJ **2020**, pp. 1–3.

[72] C. Bower, E. Menard, P. Garrou, *58th Electronic Components and Technology Conf.*, IEEE, Piscataway, NJ **2008**, pp. 1105–1109.

[73] Z. Wang, X. Shan, X. Cui, P. Tian, *J. Semicond.* **2020**, *41*, 041606.

[74] Bibl A., et al. U.S. Patent 8,426,227, **2013**.

[75] Golda, D., A. Bibl, *U.S. Patent 9,548,233*, **2017**.

[76] A. S. Holmes, S. M. Saidam, *J. Microelectromech. Syst.* **1998**, *7*, 416.

[77] V. Marinov, O. Swenson, R. Miller, F. Sarwar, Y. Atanasov, M. Semler, et al., *IEEE Trans. Compon., Packag., Manuf. Technol.* **2011**, *2*, 569.

[78] V. R. Marinov, *SID Symp. Dig. Tech. Pap.* **2018**, *49*, 692.

[79] E. Menard, K. Lee, D.-Y. Khang, R. Nuzzo, J. Rogers, *Appl. Phys. Lett.* **2004**, *84*, 5398.

[80] C. A. Bower, M. A. Meitl, S. Bonafede, D. Gomez, *65th Electronic Components and Technology Conference (ECTC)*, IEEE, Piscataway, NJ **2015**, pp. 963–967.

[81] K. Sasaki, et al. U.S. Patent. 10,418,527, **2019**.

[82] H.-J. Yeh, J. S. Smith, *IEEE Photonics Technol. Lett.* **1994**, *6*, 706.

[83] H. O. Jacobs, A. R. Tao, A. Schwartz, D. H. Gracias, G. M. Whitesides, *Science* **2002**, *296*, 323.

[84] A. Bibl, J. A. Higginson, H.-H. Hu, H.-f. S. Law, *WO2013119671A1*, **2017**.

[85] P. Delaporte, A.-P. Alloncle, *Opt. Laser Technol.* **2016**, *78*, 33.

[86] J. Li, G. Yan, B. Luo, Z. Liu, *SID Symp. Dig. Tech. Pap.* **2020**, *51*, 125.

[87] Schuele, P. J., et al. U.S. Patent 9,825,202, **2017**.

[88] J.-H. Kim, B.-C. Kim, D.-W. Lim, B.-C. Shin, *J. Mech. Sci. Technol.* **2019**, *33*, 5321.

[89] M. A. Meitl, Z.-T. Zhu, V. Kumar, K. J. Lee, X. Feng, Y. Y. Huang, et al., *Nat. Mater.* **2006**, *5*, 33.

[90] S. H. Ahn, L. J. Guo, *ACS Nano* **2009**, *3*, 2304.

[91] B. K. Sharma, B. Jang, J. E. Lee, S. H. Bae, T. W. Kim, H. J. Lee, et al., *Adv. Funct. Mater.* **2013**, *23*, 2024.

[92] X. Feng, M. A. Meitl, A. M. Bowen, Y. Huang, R. G. Nuzzo, J. A. Rogers, *Langmuir* **2007**, *23*, 12555.

[93] J. D. Eisenhaure, S. I. Rhee, M. Ala'a, A. Carlson, P. M. Ferreira, S. Kim, *J. Microelectromech. Syst.* **2014**, *23*, 1012.

[94] E. J. Radauscher, M. Meitl, C. Prevatte, S. Bonafede, R. Rotzoll, D. Gomez, et al., *Proc. SPIE* **2017**, *10124*, 1012418.

[95] H. Lu, W. Guo, C. Su, X. Li, Y. Lu, Z. Chen, et al., *IEEE J. Electron Devices Soc.* **2020**, *8*, 554.

[96] J. J. Talghader, J. K. Tu, J. S. Smith, *IEEE Photonics Technol. Lett.* **1995**, *7*, 1321.

[97] E. Saeedi, S. S. Kim, B. A. Parviz, *20th Int. Conf. Micro Electro Mechanical Systems (MEMS)*, IEEE, Piscataway, NJ **2007**, pp. 755–758.

[98] S. Cho, D. Lee, S. Kwon, *20th Int. Conf. Solid-State Sensors, Actuators and Microsystems & Eurosensors XXXIII (TRANSDUCERS & EUROSENSORS XXXIII)*, IEEE, Piscataway, NJ **2019** pp. 402–404.

[99] X. Liu, C. Tong, X. Luo, W. Li, Z. Liu, *SID Symp. Dig. Tech. Pap.* **2019**, *50*, 775.

[100] M. Choi, B. Jang, W. Lee, S. Lee, T. W. Kim, H. J. Lee, et al., *Adv. Funct. Mater.* **2017**, *27*, 1606005.

[101] S.-I. Park, Y. Xiong, R.-H. Kim, P. Elvikis, M. Meitl, D.-H. Kim, et al., *Science* **2009**, *325*, 977.

[102] I.-H. Jeon, J.-S. Yu, B.-G. Ju, *Inf. Disp.* **2018**, *19*, 41.

[103] J. H. Park, D. Y. Kim, E. F. Schubert, J. Cho, J. K. Kim, *ACS Energy Lett.* **2018**, *3*, 655.

[104] C. Li, Z. Ji, J. Li, M. Xu, H. Xiao, X. Xu, *Sci. Rep.* **2017**, *7*, 15301.

[105] M. Usman, M. Munsif, U. Mushtaq, A.-R. Anwar, N. Muhammad, *Crit. Rev. Solid State Mater. Sci.* **2021**, *46*, 450.

[106] M. G. Craford, *IEEE Circuits Devices Mag.* **1992**, *8*, 24.

[107] M. H. Crawford, *IEEE J. Sel. Top. Quantum Electron.* **2009**, *15*, 1028.

[108] S. Zhang, J. Zhang, J. Gao, X. Wang, C. Zheng, M. Zhang, et al., *Photonics Res.* **2020**, *8*, 1671.

[109] M. A. Der Maur, A. Pecchia, G. Penazzi, W. Rodrigues, A. Di Carlo, *Phys. Rev. Lett.* **2016**, *116*, 027401.

[110] M.-H. Kim, M. F. Schubert, Q. Dai, J. K. Kim, E. F. Schubert, J. Piprek, et al., *Appl. Phys. Lett.* **2007**, *91*, 183507.

[111] K. Hiramatsu, Y. Kawaguchi, M. Shimizu, N. Sawaki, T. Zheleva, R. F. Davis, et al., *MRS Internet J. Nitride Semicond. Res.* **1997**, *2*, 11.

[112] S. Pereira, M. Correia, E. Pereira, K. O'donnell, C. Trager-Cowan, F. Sweeney, et al., *Phys. Rev. B* **2001**, *64*, 205311.

[113] T. Langer, H. Jönen, A. Kruse, H. Bremers, U. Rossow, A. Hangleiter, *Appl. Phys. Lett.* **2013**, *103*, 022108.

[114] F.-P. Massabuau, M. J. Davies, F. Oehler, S. Pamenter, E. Thrush, M. J. Kappers, et al., *Appl. Phys. Lett.* **2014**, *105*, 112110.

[115] T. Takeuchi, S. Sota, M. Katsuragawa, M. Komori, H. Takeuchi, H. Amano, et al., *Jpn. J. Appl. Phys.* **1997**, *36*, L382.

[116] J. S. Im, H. Kollmer, J. Off, A. Sohmer, F. Scholz, A. Hangleiter, *Phys. Rev. B* **1998**, *57*, R9435.

[117] M. Usman, A.-R. Anwar, M. Munsif, S. Malik, N. U. Islam, *Superlattices Microstruct.* **2019**, *135*, 106271.

[118] S. Łepkowski, T. Suski, P. Perlin, V. Y. Ivanov, M. Godlewski, N. Grandjean, et al., *J. Appl. Phys.* **2002**, *91*, 9622.

[119] D. J. Lockwood, *J. Mater. Sci.: Mater. Electron.* **2009**, *20*, 235.

[120] J. J. Wierer Jr, N. Tansu, *Laser Photonics Rev.* **2019**, *13*, 1900141.

[121] F. Gou, E. L. Hsiang, G. Tan, Y. F. Lan, C. Y. Tsai, S. T. Wu, *J. Soc. Inf. Disp.* **2019**, *27*, 199.

[122] V. W. Lee, N. Twu, I. Kymissis, *Inf. Disp.* **2016**, *32*, 16.

[123] Z. Chen, S. Yan, C. Danesh, *J. Phys. D: Appl. Phys.* **2021**, *54*, 123001.

[124] T. Sharma, E. Towe, *Appl. Phys. Lett.* **2010**, *96*, 191105.

[125] J. Zhang, N. Tansu, *J. Appl. Phys.* **2011**, *110*, 113110.

[126] J. Pal, M. Migliorato, C.-K. Li, Y.-R. Wu, B. Crutchley, I. Marko, et al., *J. Appl. Phys.* **2013**, *114*, 073104.

[127] J. Däubler, T. Passow, R. Aidam, K. Köhler, L. Kirste, M. Kunzer, et al., *Appl. Phys. Lett.* **2014**, *105*, 111111.

[128] A. Even, G. Laval, O. Ledoux, P. Ferret, D. Sotta, E. Guiot, et al., *Appl. Phys. Lett.* **2017**, *110*, 262103.

[129] S. S. Pasayat, C. Gupta, M. S. Wong, Y. Wang, S. Nakamura, S. P. Denbaars, et al., *Appl. Phys. Lett.* **2020**, *116*, 111101.

[130] S. S. Pasayat, C. Gupta, M. S. Wong, R. Ley, M. J. Gordon, S. P. DenBaars, et al., *Appl. Phys. Express* **2020**, *14*, 011004.

[131] C. A. Fabien, B. P. Gunning, W. A. Doolittle, A. M. Fischer, Y. O. Wei, H. Xie, et al., *J. Cryst. Growth* **2015**, *425*, 115.

[132] J. Grandal, J. Pereiro, A. Bengoechea-Encabo, S. Fernandez-Garrido, M. A. Sánchez-García, E. Muñoz, et al., *Appl. Phys. Lett.* **2011**, *98*, 061901.

[133] S. Valdueza-Felip, L. Rigutti, F. Naranjo, P. Ruterana, J. Mangeney, F. H. Julien, et al., *Appl. Phys. Lett.* **2012**, *101*, 062109.

[134] C. E. Reilly, C. Lund, S. Nakamura, U. K. Mishra, S. P. DenBaars, S. Keller, *Appl. Phys. Lett.* **2019**, *114*, 241103.

[135] S. Łepkowski, W. Bardyszewski, *Sci. Rep.* **2018**, *8*, 15403.

[136] M. Miao, Q. Yan, C. Van de Walle, W. Lou, L. Li, K. Chang, *Phys. Rev. Lett.* **2012**, *109*, 186803.

[137] S. Łepkowski, W. Bardyszewski, *J. Phys.: Condens. Matter* **2016**, *29*, 055702.

[138] S. P. Łepkowski, W. Bardyszewski, *J. Phys.: Condens. Matter* **2017**, *29*, 195702.

[139] W. Bardyszewski, D. Rodak, S. Łepkowski, *EPL* **2017**, *118*, 27001.

[140] G. Hu, Y. Zhang, L. Li, Z. L. Wang, *ACS Nano* **2018**, *12*, 779.

[141] M. Dan, G. Hu, L. Li, Y. Zhang, *Nano Energy* **2018**, *50*, 544.

[142] I. Vasileiadis, L. Lymperakis, A. Adikimenakis, A. Gkotinakos, V. Devulapalli, C. Liebscher, et al., *Sci. Rep.* **2021**, *11*, 20606.

[143] H.-V. Han, H.-Y. Lin, C.-C. Lin, W.-C. Chong, J.-R. Li, K.-J. Chen, et al., *Opt. Express* **2015**, *23*, 32504.

[144] A. Rudorfer, M. Tscherner, C. Palfinger, F. Reil, P. Hartmann, I. E. Seferis, et al., *Proc. SPIE* **2016**, *9954*, 99540E.

[145] M. Singh, H. M. Haverinen, P. Dhagat, G. E. Jabbour, *Adv. Mater.* **2010**, *22*, 673.

[146] K. J. Chen, H. C. Chen, K. A. Tsai, C. C. Lin, H. H. Tsai, S. H. Chien, et al., *Adv. Funct. Mater.* **2012**, *22*, 5138.

[147] J. Han, J. Choi, A. Piquette, M. Hannah, M. Anc, M. Galvez, et al., *ECS J. Solid State Sci. Technol.* **2012**, *2*, R3138.

[148] D.-C. Chen, Z.-G. Liu, Z.-H. Deng, C. Wang, Y.-G. Cao, Q.-L. Liu, *Rare Met.* **2014**, *33*, 348.

[149] T. Tao, T. Zhi, X. Cen, B. Liu, Q. Wang, Z. Xie, et al., *IEEE Photonics J.* **2018**, *10*, 8201608.

[150] J. McKittrick, L. E. Shea-Rohwer, *J. Am. Ceram. Soc.* **2014**, *97*, 1327.

[151] G. B. Nair, H. Swart, S. Dhoble, *Prog. Mater. Sci.* **2020**, *109*, 100622.

[152] A. Rapaport, J. Milliez, M. Bass, A. Cassanho, H. Jenssen, *J. Disp. Technol.* **2006**, *2*, 68.

[153] B. Xie, R. Hu, X. Luo, *J. Electron. Packag.* **2016**, *138*, 020803.

[154] S. Coe-Sullivan, W. Liu, P. Allen, J. S. Steckel, *ECS J. Solid State Sci. Technol.* **2012**, *2*, R3026.

[155] H. Mattoussi, J. M. Mauro, E. R. Goldman, G. P. Anderson, V. C. Sundar, F. V. Mikulec, et al., *J. Am. Chem. Soc.* **2000**, *122*, 12142.

[156] S. B. Brichkin, V. F. Razumov, *Russ. Chem. Rev.* **2016**, *85*, 1297.

[157] Y. Shirasaki, G. J. Supran, M. G. Bawendi, V. Bulović, *Nat. Photonics* **2013**, *7*, 13.

[158] F. Yuan, Z. Wang, X. Li, Y. Li, Z. a. Tan, L. Fan, et al., *Adv. Mater.* **2017**, *29*, 1604436.

[159] H. Song, S. Lee, *Nanotechnology* **2007**, *18*, 255202.

[160] H. L. Kang, J. Kang, J. K. Won, S. M. Jung, J. Kim, C. H. Park, et al., *Adv. Opt. Mater.* **2018**, *6*, 1701335.

[161] R. Palankar, N. Medvedev, A. Rong, M. Delcea, *ACS Nano* **2013**, *7*, 4617.

[162] Y. L. Kong, I. A. Tamargo, H. Kim, B. N. Johnson, M. K. Gupta, T.-W. Koh, et al., *Nano Lett.* **2014**, *14*, 7017.

[163] V. R. Manfrinato, L. Zhang, D. Su, H. Duan, R. G. Hobbs, E. A. Stach, et al., *Nano Lett.* **2013**, *13*, 1555.

[164] P. Richner, P. Galliker, T. Lendenmann, S. J. Kress, D. K. Kim, D. J. Norris, et al., *ACS Photonics* **2016**, *3*, 754.

[165] Z. Luo, D. Xu, S.-T. Wu, *J. Disp. Technol.* **2014**, *10*, 526.

[166] H. Chen, J. He, S.-T. Wu, *IEEE J. Sel. Top. Quantum Electron.* **2017**, *23*, 1900611.

[167] A. Trindade, Ph.D. Thesis, University of Strathclyde, **2015**.

[168] J. M. Santos, B. E. Jones, P. J. Schlosser, S. Watson, J. Herrnsdorf, B. Guilhabert, et al., *Semicond. Sci. Technol.* **2015**, *30*, 035012.

[169] H.-Y. Lin, C.-W. Sher, D.-H. Hsieh, X.-Y. Chen, H.-M. P. Chen, T.-M. Chen, et al., *Photonics Res.* **2017**, *5*, 411.

[170] F. Gou, E.-L. Hsiang, G. Tan, Y.-F. Lan, C.-Y. Tsai, S.-T. Wu, *Crystals* **2019**, *9*, 39.

[171] C. Jiang, Z. Zhong, B. Liu, Z. He, J. Zou, L. Wang, et al., *ACS Appl. Mater. Interfaces* **2016**, *8*, 26162.

[172] L. Cui, J. Zhang, X. Zhang, L. Huang, Z. Wang, Y. Li, et al., *ACS Appl. Mater. Interfaces* **2012**, *4*, 2775.

[173] Y. Liu, F. Li, Z. Xu, C. Zheng, T. Guo, X. Xie, et al., *ACS Appl. Mater. Interfaces* **2017**, *9*, 25506.

[174] A. Gao, J. Yan, Z. Wang, P. Liu, D. Wu, X. Tang, et al., *Nanoscale* **2020**, *12*, 2569.

[175] G.-S. Chen, B.-Y. Wei, C.-T. Lee, H.-Y. Lee, *IEEE Photonics Technol. Lett.* **2017**, *30*, 262.

[176] Z. Hens, I. Moreels, *J. Mater. Chem.* **2012**, *22*, 10406.

[177] J. Osinski, P. Palomaki, *SID Symp. Dig. Tech. Pap.* **2019**, *50*, 34.

[178] E. Lee, R. Tangirala, A. Smith, A. Carpenter, C. Hotz, H. Kim, et al., *SID Symp. Dig. Tech. Pap.* **2018**, *49*, 525.

[179] S.-Y. Chu, H.-Y. Wang, C-T. Lee, H.-Y. Lee, K.-L. Laing, W.-H. Kuo, et al., *Coatings* **2020**, *10*, 436.

[180] J. J. Wierer, A. David, M. M. Megens, *Nat. Photonics* **2009**, *3*, 163.

[181] C. Wiesmann, K. Bergenek, N. Linder, U. T. Schwarz, *Laser Photonics Rev.* **2009**, *3*, 262.

[182] C. Krishnan, M. Brossard, K.-Y. Lee, J.-K. Huang, C.-H. Lin, H.-C. Kuo, et al., *Optica* **2016**, *3*, 503.

[183] F. Zhang, J. Liu, G. You, C. Zhang, S. E. Mohney, M. J. Park, et al., *Opt. Express* **2012**, *20*, A333.

[184] A. R. Clapp, I. L. Medintz, H. Mattoussi, *ChemPhysChem* **2006**, *7*, 47.

[185] S. Chanyawadee, P. G. Lagoudakis, R. T. Harley, M. D. Charlton, D. V. Talapin, H. W. Huang, et al., *Adv. Mater.* **2010**, *22*, 602.

[186] C. Zhao, T. K. Ng, R. T. ElAfandy, A. Prabaswara, G. B. Consiglio, I. A. Ajia, et al., *Nano Lett.* **2016**, *16*, 4616.

[187] S.-W. Wang, K.-B. Hong, Y.-L. Tsai, C.-H. Teng, A.-J. Tzou, Y.-C. Chu, et al., *Sci. Rep.* **2017**, *7*, 42962.

[188] S.-W. H. Chen, C.-C. Shen, T. Wu, Z.-Y. Liao, L.-F. Chen, J.-R. Zhou, et al., *Photonics Res.* **2019**, *7*, 416.

[189] M. Achermann, M. A. Petruska, S. Kos, D. L. Smith, D. D. Koleske, V. I. Klimov, *Nature* **2004**, *429*, 642.

[190] D. A. Hines, M. A. Becker, P. V. Kamat, *J. Phys. Chem. C* **2012**, *116*, 13452.

[191] H. C. Park, S. Gong, Y. H. Cho, *Small* **2017**, *13*, 1701805.

[192] K. B. Bae, W. W. Lee, H. Y. Song, J. H. Yun, A. Y. Polyakov, I. H. Lee, *Phys. Status Solidi* **2018**, *215*, 1700644.

[193] J. Li, Y. Tang, Z. Li, X. Ding, L. Rao, B. Yu, *Opt. Lett.* **2019**, *44*, 90.

[194] D.-S. Kim, S.-Y. Kim, J.-H. Jung, S.-Y. Shin, *Electronic Imaging* **2018**, *2018*, 185.

[195] J.-H. Kang, B. Li, T. Zhao, M. A. Johar, C.-C. Lin, Y.-H. Fang, et al., *ACS Appl. Mater. Interfaces* **2020**, *12*, 30890.

[196] J.-H. Kang, J. Han, *SID Symp. Dig. Tech. Pap.* **2019**, *50*, 914.

[197] D. J. Durian, *Phys. Rev. E* **1994**, *50*, 857.

[198] J. Zhu, D. Pine, D. Weitz, *Phys. Rev. A* **1991**, *44*, 3948.

[199] O. L. Muskens, J. G. Rivas, R. E. Algra, E. P. Bakkers, A. Lagendijk, *Nano Lett.* **2008**, *8*, 2638.

[200] J. Frank, D. Vanmaekelbergh, J. van de Lagemaat, A. Lagendijk, *Science* **1999**, *284*, 141.

[201] C. Zhang, S. H. Park, D. Chen, D.-W. Lin, W. Xiong, H.-C. Kuo, et al., *ACS Photonics* **2015**, *2*, 980.

[202] P. M. Johnson, B. P. Bret, J. G. Rivas, J. J. Kelly, A. Lagendijk, *Phys. Rev. Lett.* **2002**, *89*, 243901.

[203] W. Mei, Z. Zhang, A. Zhang, D. Li, X. Zhang, H. Wang, et al., *Nano Res.* **2020**, *13*, 2485.

Abdur Rehman Anwar completed his master's degree in engineering sciences from Ghulam Ishaq Khan Institute of Engineering Sciences and Technology (GIK Institute), Topi, Swabi, Pakistan in 2020. He has won a GIK Institute Fellowship and Graduate Assistantship Award for master's studies from 2018 to 2020, and an Institutional Gold Medal Award (from GIK Institute) for the overall best academic performance of the institute by Dr. Arif Alvi, President of Pakistan. His research focuses on III–V semiconductor materials for light-emitting applications.

Dr. Muhammad Tariq Sajjad is a senior Lecturer in the School of Engineering at London South Bank University (UK) where he set up his own group "Energy Engineering and Materials Devices." The group research interests are to understand the physics of semiconductor materials and devices, with the aim of improving them. In recognition of his contribution to the field, the Royal Society of Chemistry (RSC, UK) has recognized him as one of the emerging investigators in 2020. He received his M.Sc. and Ph.D., both from Advanced Technology Institute, University of Surrey, UK.